Journal of Applied Mathematics and Physics, 2019, 7, 2231-2264
https://www.scirp.org/journal/jamp
ISSN Online: 2327-4379
ISSN Print: 2327-4352

The Classical Hall Effect in Multiply-Connected Plane Regions Part II: Spiral Current Streamlines

Udo Ausserlechner

Department of Sense and Control, Infineon Technologies AG, Villach, Austria
Email: udo.ausserlechner@infineon.com

How to cite this paper: Ausserlechner, U. (2019) The Classical Hall Effect in Multiply-Connected Plane Regions Part II: Spiral Current Streamlines. *Journal of Applied Mathematics and Physics*, **7**, 2231-2264.
https://doi.org/10.4236/jamp.2019.710153

Received: August 26, 2019
Accepted: October 8, 2019
Published: October 11, 2019

Abstract

Multiply-connected Hall plates show different phenomena than singly connected Hall plates. In part I (published in Journal of Applied Physics and Mathematics), we discussed topologies where a stream function can be defined, with special reference to Hall/Anti-Hall bar configurations. In part II, we focus on topologies where no conventional stream function can be defined, like Corbino disks. If current is injected and extracted at different boundaries of a multiply-connected conductive region, the current density shows spiral streamlines at strong magnetic field. Spiral streamlines also appear in simply-connected Hall plates when current contacts are located in their interior instead of their boundary, particularly if the contacts are very small. Spiral streamlines and circulating current are studied for two complementary planar device geometries: either all boundaries are conducting or all boundaries are insulating. The latter case means point current contacts and it can be treated similarly to singly connected Hall plates with peripheral contacts through the definition of a so-called loop stream function. This function also establishes a relation between Hall plates with complementary boundary conditions. The theory is explained by examples.

Keywords

Circulating Current, Corbino Disk, Corbino Images, Corbinotron, Doubly Connected, Hall Plate, Loop Current, Multiply Connected, Non-Peripheral Contacts, Reverse Magnetic Field Reciprocity, Spiral Streamlines, Stream Function

1. Introduction

Part II of this paper largely builds on part I, where we studied the stream func-

tion of plane multiply-connected Hall plates [1]. In part I, we found that in the absence of spiral streamlines, the stream function obeys particularly simple rules when all boundaries are insulating except for the point-sized contacts. Then the stream function is independent of the applied magnetic field and it is linearly proportional to the Hall potential. Thus, there is no Hall voltage between points on the same current streamline. In the following, we will see that for a large group of Hall plates, no classical stream function exists. As a consequence, such devices show entirely different behavior with the most striking new feature being spiral current streamlines. Such spiral current streamlines were known in multiply-connected Hall plates where all boundaries were contacts [2] [3]. A well-known example of such a topology is the Corbino disk, which maximizes the magneto-resistance effect. However, there are numerous equivalent shapes—most of them are multiply-connected. This was already known at a very early time [2]. In [3], it was proven that there is no Hall voltage between any contacts of such a device. In [2], the author explicitly states that in such kinds of devices, the equipotential lines remain unaltered by the application of an external magnetic field. He also gave a general expression for the magnitude of the circulating currents that show up in these devices—we will pick up this thread in **Section 3** after some basic definitions in **Section 2**. In **Section 4**, we discuss the converse case, *i.e.*, multiply-connected Hall plates with insulating boundaries and point-sized contacts with internal current sources (the case without internal current sources was treated in part I). No theory exists on this kind of Hall plates so far. Finally, **Section 5** summarizes all rules of parts I and II for convenient reference. Some symmetries and similarities will become apparent. **Appendices A** and **B** give analytical calculations of the current density in singly- and doubly-connected regions with insulating boundaries and spiral current streamlines. There, current is injected near the center and flows to a point on the unit circle. **Appendix C** deals with a specific detail of reverse magnetic field reciprocity for multiply-connected regions in two dimensions.

2. Assumptions and Basic Definitions

In this part II, the same assumptions and definitions apply as in part I [1]. Here we repeat the important ones. We assume only negative charge carriers. Then the Hall effect in a plane Hall plate in the (x, y)-plane with small thickness t_H is described by

$$\boldsymbol{E} = \rho\boldsymbol{J} + \rho\mu_H \boldsymbol{J}\times\boldsymbol{B}_a \quad \Leftrightarrow \quad \boldsymbol{J} = \frac{\boldsymbol{E} - \mu_H \boldsymbol{E}\times\boldsymbol{B}_a}{\rho\left(1+\mu_H^2 B_{a,z}^2\right)} \tag{1}$$

with the externally applied magnetic field $\boldsymbol{B}_a = B_{a,z}\boldsymbol{n}_z$, the specific ohmic resistivity $\rho > 0$, and the Hall mobility $\mu_H > 0$. $\boldsymbol{J}\times\boldsymbol{B}_a$ denotes the vector product of $\boldsymbol{J}$ and $\boldsymbol{B}_a$. This work is limited to the linear case, where ρ and μ_H are constant versus $\boldsymbol{E}$ and $\boldsymbol{B}_a$. We decompose the potential ϕ, the electric field $\boldsymbol{E}$, and the current density $\boldsymbol{J}$ into even and odd functions of the applied magnetic field. Thereby we hold either the supply current or voltage constant

while changing the polarity of the applied magnetic field.

$$\phi\left(\boldsymbol{r},B_{a,z}\right)=\phi_{\text{even}}\left(\boldsymbol{r},B_{a,z}\right)+\phi_{\text{odd}}\left(\boldsymbol{r},B_{a,z}\right) \tag{2a}$$

$$\phi_{\text{even}}\left(\boldsymbol{r},B_{a,z}\right)=\frac{\phi\left(\boldsymbol{r},B_{a,z}\right)+\phi\left(\boldsymbol{r},-B_{a,z}\right)}{2} \tag{2b}$$

$$\phi_{\text{odd}}\left(\boldsymbol{r},B_{a,z}\right)=\phi_{H}\left(\boldsymbol{r},B_{a,z}\right)=\frac{\phi\left(\boldsymbol{r},B_{a,z}\right)-\phi\left(\boldsymbol{r},-B_{a,z}\right)}{2} \tag{2c}$$

$$\boldsymbol{E}\left(\boldsymbol{r},B_{a,z}\right)=\boldsymbol{E}_{\text{even}}\left(\boldsymbol{r},B_{a,z}\right)+\boldsymbol{E}_{\text{odd}}\left(\boldsymbol{r},B_{a,z}\right)=-\nabla\phi \tag{3a}$$

$$\boldsymbol{E}_{\text{even}}\left(\boldsymbol{r},B_{a,z}\right)=\frac{\boldsymbol{E}\left(\boldsymbol{r},B_{a,z}\right)+\boldsymbol{E}\left(\boldsymbol{r},-B_{a,z}\right)}{2}=-\nabla\phi_{\text{even}} \tag{3b}$$

$$\boldsymbol{E}_{\text{odd}}\left(\boldsymbol{r},B_{a,z}\right)=\boldsymbol{E}_{H}\left(\boldsymbol{r},B_{a,z}\right)=\frac{\boldsymbol{E}\left(\boldsymbol{r},B_{a,z}\right)-\boldsymbol{E}\left(\boldsymbol{r},-B_{a,z}\right)}{2}=-\nabla\phi_{H} \tag{3c}$$

$$\boldsymbol{J}\left(\boldsymbol{r},B_{a,z}\right)=\boldsymbol{J}_{\text{even}}\left(\boldsymbol{r},B_{a,z}\right)+\boldsymbol{J}_{\text{odd}}\left(\boldsymbol{r},B_{a,z}\right) \tag{4a}$$

$$\boldsymbol{J}_{\text{even}}\left(\boldsymbol{r},B_{a,z}\right)=\frac{\boldsymbol{J}\left(\boldsymbol{r},B_{a,z}\right)+\boldsymbol{J}\left(\boldsymbol{r},-B_{a,z}\right)}{2} \tag{4b}$$

$$\boldsymbol{J}_{\text{odd}}\left(\boldsymbol{r},B_{a,z}\right)=\frac{\boldsymbol{J}\left(\boldsymbol{r},B_{a,z}\right)-\boldsymbol{J}\left(\boldsymbol{r},-B_{a,z}\right)}{2} \tag{4c}$$

The odd potential is also called Hall potential. The difference in Hall potential at two test points on two contacts is called Hall voltage. The odd electric field is also called the Hall electric field. All odd functions vanish at zero applied magnetic field due to their definition. We denote all even functions at zero applied magnetic fields with an index 0.

$$\phi\left(\boldsymbol{r},0\right)=\phi_{\text{even}}\left(\boldsymbol{r},0\right)=\phi_{0}\left(\boldsymbol{r}\right) \tag{5a}$$

$$\boldsymbol{E}\left(\boldsymbol{r},0\right)=\boldsymbol{E}_{\text{even}}\left(\boldsymbol{r},0\right)=\boldsymbol{E}_{0}\left(\boldsymbol{r}\right) \tag{5b}$$

$$\boldsymbol{J}\left(\boldsymbol{r},0\right)=\boldsymbol{J}_{\text{even}}\left(\boldsymbol{r},0\right)=\boldsymbol{J}_{0}\left(\boldsymbol{r}\right) \tag{5c}$$

In the entire Hall plate, the electric field vectors $\boldsymbol{E}$ are rotated by the Hall angle θ_H against the current density vectors $\boldsymbol{J}$. From (1), we get $\tan\theta_H=\mu_H B_{a,z}$. Inserting (1) for both polarities of the applied magnetic field into (3b, c) and (4b, c) gives relations between even and odd vector fields.

$$\boldsymbol{E}_{\text{odd}}=\boldsymbol{E}_{H}=\rho\boldsymbol{J}_{\text{odd}}+\rho\mu_{H}\boldsymbol{J}_{\text{even}}\times\boldsymbol{B}_{a} \tag{6a}$$

$$\boldsymbol{E}_{\text{even}}=\rho\boldsymbol{J}_{\text{even}}+\rho\mu_{H}\boldsymbol{J}_{\text{odd}}\times\boldsymbol{B}_{a} \tag{6b}$$

$$\boldsymbol{J}_{\text{odd}}=\frac{\boldsymbol{E}_{\text{odd}}-\mu_{H}\boldsymbol{E}_{\text{even}}\times\boldsymbol{B}_{a}}{\rho\left(1+\mu_{H}^{2}B_{a,z}^{2}\right)} \tag{6c}$$

$$\boldsymbol{J}_{\text{even}}=\frac{\boldsymbol{E}_{\text{even}}-\mu_{H}\boldsymbol{E}_{\text{odd}}\times\boldsymbol{B}_{a}}{\rho\left(1+\mu_{H}^{2}B_{a,z}^{2}\right)} \tag{6d}$$

Instead of computing the electric field and the current density directly, one commonly uses the electric potential $\phi(\boldsymbol{r})$ or the stream function $\psi(\boldsymbol{r})$. However, in **Section 5** of part I [1], we saw that the stream function works only

for a limited class of Hall plates, namely the ones *without* internal current sources: $\boldsymbol{J}=-\rho^{-1}\nabla\times\psi\boldsymbol{n}_z$ holds only if $\oint\boldsymbol{J}\cdot\boldsymbol{n}\mathrm{d}s=0$ along all loops within the multiply-connected domain (see **Section 5** of part I). In this part II, we address Hall plates *with* internal current sources and therefore we have to use the potential ϕ instead of the conventional stream function ψ.

In the stationary case Faraday's law of electromagnetic induction $\nabla\times\boldsymbol{E}=-\partial\boldsymbol{B}/\partial t\to\boldsymbol{0}$ means that the electric field can be expressed as a gradient of a scalar potential $\boldsymbol{E}=-\nabla\phi$ (cf. (3a)). On the other hand, stationary current flow implies that the amount of electricity entering any volume element inside a Hall plate must equal that leaving it, thus $\nabla\cdot\boldsymbol{J}=0$. Hereby we cut out all current-carrying contacts on the boundaries and inside the Hall effect region (see **Section 4**). Letting nabla operate on (1) and using these results leads to $\nabla\cdot\boldsymbol{E}=0$. It means that under stationary conditions net charge density vanishes everywhere inside a homogeneous Hall plate. From $\nabla\cdot\boldsymbol{E}=0$ it follows the Laplace equation $\nabla^2\phi=0$ for the potential. With (2b, c) also ϕ_{even} and ϕ_H are solutions of the Laplace equation.

3. Plane Hall Plates Where All Boundaries Are Contacts

On the boundary of a general Hall plate, we distinguish between insulating boundaries and contacts. On the contacts, the value of ϕ is either forced by external voltage sources or it follows from a fixed current into the contact (either $\pm I_{\text{supply}}$ in the supply contacts or zero in the sense contacts). On the insulating boundary, there is no normal current density and therefore the electric field is rotated by the Hall angle against the tangent on the boundary. For the potential, this gives an unusual boundary condition $\partial\phi/\partial n=(\tan\theta_H)\partial\phi/\partial t$ [4]. Here $\partial\phi/\partial n=\boldsymbol{n}\cdot\nabla\phi$ means derivation in the direction $\boldsymbol{n}$ normal to the boundary and $\partial\phi/\partial t=\boldsymbol{t}\cdot\nabla\phi$ means derivation in the direction $\boldsymbol{t}$ tangential to the boundary with $\boldsymbol{n}\cdot\boldsymbol{n}=1$, $\boldsymbol{t}\cdot\boldsymbol{t}=1$, and $\boldsymbol{n}\cdot\boldsymbol{t}=0$. The magnetic field dependence of the potential enters via $\tan\theta_H=\mu_H B_{a,z}$ in the boundary condition, it does not enter via Laplace's equation.

Suppose a Hall plate in two-dimensional space with an arbitrary number of holes. On its outer perimeter and on the hole boundaries it is bounded by contacts only, having no insulating boundary. If all contacts are tied to voltage sources, then the boundary conditions contain no magnetic field dependence any more. Thus *the electric potential and the electric field in these Hall plates are independent of any applied magnetic field*. This means:

$$\phi=\phi_0=\phi_{\text{even}}\quad\Rightarrow\quad\boldsymbol{E}_{\text{even}}=\boldsymbol{E}_0 \tag{7a}$$

$$\Rightarrow\quad\phi_H=0\quad\Rightarrow\quad\boldsymbol{E}_H=\boldsymbol{0} \tag{7b}$$

The Hall potential ϕ_H *and the Hall electric field* $\boldsymbol{E}_H$ *vanish everywhere in these Hall plates*. Inserting (7a, b) into (6c, d) and (1) with $\boldsymbol{E}_0/\rho=\boldsymbol{J}_0$ gives:

$$\boldsymbol{J}_{\text{odd}}=\frac{-\mu_H\boldsymbol{J}_0\times\boldsymbol{B}_a}{1+\mu_H^2B_{a,z}^2} \tag{8a}$$

$$\boldsymbol{J}_{\text{even}} = \frac{\boldsymbol{J}_0}{1+\mu_H^2 B_{a,z}^2} \tag{8b}$$

$$\boldsymbol{J} = \frac{\boldsymbol{J}_0 - \mu_H \boldsymbol{J}_0 \times \boldsymbol{B}_a}{1+\mu_H^2 B_{a,z}^2} \tag{8c}$$

It holds $\boldsymbol{J}_{\text{odd}} = -\mu_H \boldsymbol{J}_{\text{even}} \times \boldsymbol{B}_a$. In particular $\boldsymbol{J}_{\text{odd}} \perp \boldsymbol{J}_{\text{even}}$ and $\boldsymbol{J}_{\text{even}} \| \boldsymbol{J}_0$. We can solve (8c) for $\boldsymbol{J}_0$. Alternatively, from (7a, b) we can simply say $\boldsymbol{E}_0 = \boldsymbol{E}$ and replace $\boldsymbol{E}$ by the left equation in (1). The result is:

$$\boldsymbol{J}_0 = \boldsymbol{J} + \mu_H \boldsymbol{J} \times \boldsymbol{B}_a \tag{9a}$$

Therefore $\boldsymbol{J}_0$ and $\boldsymbol{J}$ are rotated by the Hall angle and scaled in magnitude.

$$|\boldsymbol{J}_0| = \sqrt{1+\mu_H^2 B_{a,z}^2}\,|\boldsymbol{J}| = |\boldsymbol{J}|/\cos|\theta_H| \tag{9b}$$

This holds inside the Hall plate but also on the contacts. In other words, at fixed potentials on all contacts, the current density normal to the contacts at the applied magnetic field is smaller by the factor $(\cos\theta_H)^2$. We can relate the potentials and currents at all contacts of such a Hall plate via a resistance matrix, because the device is electrically linear: due to the superposition principle, the potential at any contact is a linear combination of currents at all contacts. Then all resistances are proportional to $(\cos\theta_H)^{-2} = 1+\mu_H^2 B_{a,z}^2$, which is an even function in $B_{a,z}$. Consequently, *the Hall voltage vanishes* also at constant supply current of the Hall plate, because it is an odd function in $B_{a,z}$ according to its definition (2c). This is identical to (7b). Zero Hall voltage was shown by Haeusler in his 1967 thesis [3]. With finite element simulations (FEM) it is straightforward to verify this on devices with multiply-connected Hall domains, where all hole boundaries are contacts on different potential. Then the current streamlines show pronounced spirals at large magnetic field (see **Figure 1(a)** & **Figure 1(b)**). However, the vanishing of Hall voltages also holds for geometries where unitary hole boundaries are split in two or more contacts at different potential. These cases are extremely challenging to study with FEM, due to insufficient meshing at the interface of contacts on the same boundary.

Furthermore, the electrical equivalent of such a Hall plate with n contacts is a pure resistor network with resistors $R_{ij} = R_{ij,0}/(\cos\theta_H)^2$ between contacts i and j with $1 \le i, j \le n$ with $i < j$. $R_{ij,0}$ is the respective resistor at zero applied magnetic fields. This gives a network with $n(n-1)/2$ resistors. Hence, the electric response of such a Hall plate with n contacts is fully described by $n(n-1)/2$ degrees of freedom. This particular group of Hall plates shows *simple reciprocity*, which means that supply current (input) and sense voltage (output) electrodes may be interchanged without any change in the output voltage. Conversely, all other Hall plates show reverse magnetic field reciprocity (RMFR [5] [6] [7]), which means that current and voltage electrodes may be interchanged, *provided the applied magnetic field is reversed*, too. Therefore, the equivalent circuit representation of Hall plates with all boundaries being electrodes is a pure resistor network, which does not comprise non-reciprocal elements like gyrators or

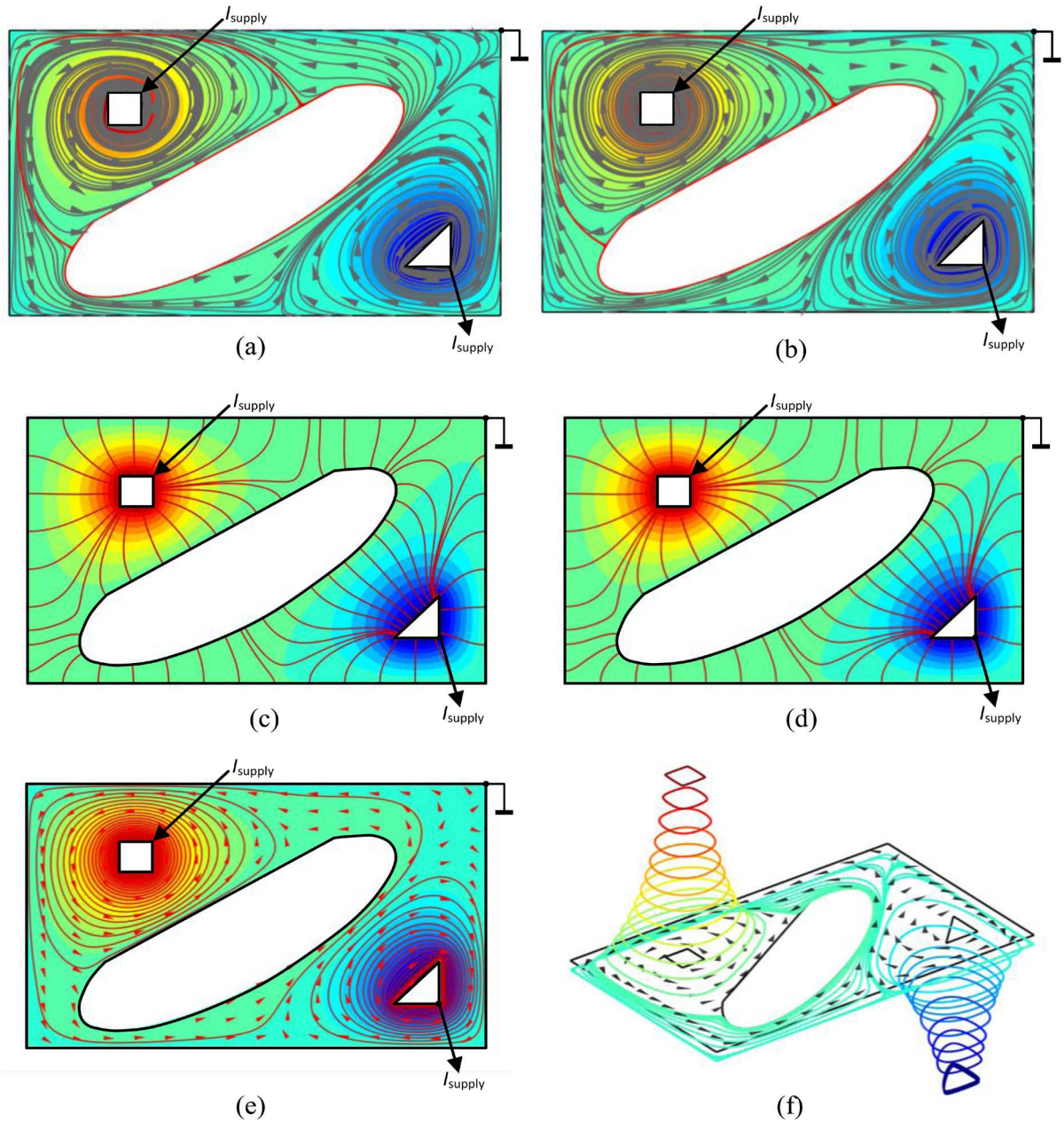

Figure 1. The same Hall effect region as in **Figure 9** of part I, but here all boundaries are electrodes drawn as solid black lines. 1 A current is input at the square hole and sunk at the triangular hole. The electrode on the perimeter is grounded for reasons of compatibility with Section 4. (a), (b) Current streamlines and cones in grey, potential in identical color map (red means 25.28 V, blue means −22.07 V) for $\mu_H B_{a,z} = 10$ in (a) and $\mu_H B_{a,z} = -10$ in (b). The red curve is an equipotential line at 1.2348 V. Note the different directions of the spiral currents in (a) and (b). ((c), (d)) Current streamlines in red, potential in identical color map (red means 0.250307 V, blue means −0.218552 V) for zero applied magnetic field in (c), whereas (d) shows the even current density $\boldsymbol{J}_{even}$ and the scaled even potential $\phi_{even}/\left(1+\mu_H^2 B_{a,z}^2\right)$ at $\mu_H B_{a,z} = 10$. The plots in (c) and (d) are perfectly identical. (e) The red streamlines and cones denote the odd current density $\boldsymbol{J}_{odd}$ and the color map is the potential at $\mu_H B_{a,z} = 10$. (f) shows the same data as (e) in a different plot: here the lines and cones denote streamlines and orientation of the odd current density $\boldsymbol{J}_{odd}$, the height above/below the Hall plate and the color-coding denote the potential at $\mu_H B_{a,z} = 10$. Obviously, the streamlines of $\boldsymbol{J}_{odd}$ are closed loops, and each loop has a unitary color at constant height, because the $\boldsymbol{J}_{odd}$ streamlines flow along equipotential lines. All displayed quantities were obtained in FEM simulations with COMSOL MULTIPHYSICS in a plane conduction model with (1).

controlled sources [8] [9]. If we supply such a Hall plate with a constant voltage source certain potentials will appear at the other (floating) contacts. If we change the applied magnetic field the ratios of resistances will remain the same and therefore the potentials at the floating contacts will also remain constant.

What happens if we supply the Hall plate with a constant current source instead of a constant voltage source? Due to the increase of resistances all potentials will rise by the same factor $\left(\cos\theta_H\right)^{-2} = \left(1+\mu_H^2 B_{a,z}^2\right)$. The Hall plate responds as if we would have supplied it with a voltage source whose voltage was increased by the same factor $1+\mu_H^2 B_{a,z}^2$. With (8a, b) this means:

$$\tilde{\boldsymbol{J}}_{\text{odd}} = -\mu_H \tilde{\boldsymbol{J}}_0 \times \boldsymbol{B}_a \quad \text{and} \quad \tilde{\boldsymbol{J}}_{\text{even}} = \tilde{\boldsymbol{J}}_0 \tag{10a}$$

$$\tilde{\phi} = \tilde{\phi}_{\text{even}} = \left(1+\mu_H^2 B_{a,z}^2\right)\tilde{\phi}_0 \quad \text{and} \quad \tilde{\phi}_H = 0 \tag{10b}$$

for constant supply current. The tilde refers to the operating condition "constant supply current" of the Hall plate with conducting boundaries. In words: *under constant supply current the even current density is constant versus applied magnetic field and the odd current density is linearly proportional to the applied magnetic field*. We will encounter the same behavior of $\boldsymbol{J}_{\text{odd}}$ and $\boldsymbol{J}_{\text{even}}$ versus applied magnetic field in Hall plates with all insulating boundaries and point sized contacts with internal current sources (see **Section 4**). **Figure 1(c)** & **Figure 1(d)** show the identities of even current density and even potential with current density and potential at zero applied magnetic field, respectively, according to (10a, b).

The equipotential lines encircle the current input contact if the contact subtends the entire closed boundary of a hole (here we ignore cases where a unitary boundary is split up into several contacts). At zero applied magnetic field, the current density vector is perpendicular to these loops ($\boldsymbol{n}\times\boldsymbol{J}_0 = \boldsymbol{0}$), but if a magnetic field is impressed on the Hall plate, the current density rotates by the Hall angle while the equipotential line remains fixed at constant supply voltage. Then the component $|\boldsymbol{J}|\sin\theta_H$ is tangential to the equipotential loop. We can integrate this current component along this loop *L*, which gives the circulation Γ around the current source.

$$\Gamma = \oint_L \boldsymbol{J}\cdot\boldsymbol{t}\mathrm{d}s = \oint_L |\boldsymbol{J}|\sin\theta_H \mathrm{d}s = \boldsymbol{n}_z \cdot \oint_L \boldsymbol{n}\times\boldsymbol{J}\mathrm{d}s \tag{11a}$$

The unit vector $\boldsymbol{t}$ points in tangential direction along the loop L such that the current contact is at its left hand side. The unit vector $\boldsymbol{n}$ is orthogonal to the equipotential lines and points away from the current contact. It holds $\boldsymbol{n}_z\times\boldsymbol{n} = \boldsymbol{t}$. From (8c) we get:

$$\boldsymbol{J} = \boldsymbol{J}_0\cos^2\theta_H - \boldsymbol{J}_0\times\boldsymbol{n}_z\cos\theta_H\sin\theta_H \tag{11b}$$

Inserting (11b) into (11a) with $\boldsymbol{n}\times\boldsymbol{J}_0 = \boldsymbol{0}$ gives the circulation:

$$\Gamma = \cos\theta_H\sin\theta_H\oint_L \boldsymbol{J}_0\cdot\boldsymbol{n}\mathrm{d}s = \cos\theta_H\sin\theta_H\frac{I_{\text{supply},0}}{t_H} = \tan\theta_H\frac{I_{\text{supply}}}{t_H} \tag{11c}$$

Thereby we used the ratio of supply currents with and without applied mag-

netic field $I_{\text{supply}}/I_{\text{supply},0}=(\cos\theta_H)^2$ at fixed supply voltage. In the integration, we used the fact that the total supply current flows out of the closed-loop L. Note that the loop L can be entirely within the conductive region, but it may also comprise portions of electrodes in a multiply-connected Hall plate. In the latter case, the loop enters and leaves the electrode in stagnation points of the current density at zero applied magnetic field (see the red 1.2348 V contour lines in **Figure 1(a)** & **Figure 1(b)**). Non-vanishing circulation means that the current streamlines are spirals around the current input electrode whenever there is a closed path around it within the conductive region. The same applies to the current output electrode (with opposite sign). If the entire outer perimeter is one supply contact, the current pattern has only one spiral pattern, otherwise, it has two spirals in opposite directions. There is no circulation and no spirals around electrodes, where no net current flows in or out. If a floating electrode encircles both current input and output contacts the circulation along it vanishes. Then this loop L can be split up in smaller loops with branching points being the stagnation points of the current density at zero magnetic field, and at least one of these smaller loops has non-vanishing circulation.

At constant supply voltage, the equipotential lines in the Hall plate are also constant versus applied magnetic field. With (8b) the even current density is orthogonal to the equipotential lines. With (8a) the odd current density is parallel to the equipotential lines. Thus, $\boldsymbol{J}_{\text{odd}}$ flows in closed loops along equipotential lines (see **Figure 1(e)**). Summing up all contributions between two fixed potentials $\phi_1<\phi_2$ at constant supply voltage gives with (8a) the respective circulating or loop current.

$$\begin{aligned} I_{\text{loop},12} &= t_H\int_1^2 \boldsymbol{J}_{\text{odd}}\cdot\boldsymbol{n}\mathrm{d}s=\frac{\mu_H B_{a,z}t_H}{1+\mu_H^2B_{a,z}^2}\int_1^2\left(\boldsymbol{n}_z\times\frac{\boldsymbol{E}_0}{\rho}\right)\cdot\boldsymbol{n}\mathrm{d}s \\ &=\frac{\mu_H B_{a,z}}{1+\mu_H^2B_{a,z}^2}\frac{t_H}{\rho}\int_1^2\mathrm{d}s\,\boldsymbol{t}\cdot\nabla\phi=\cos\theta_H\sin\theta_H\frac{\phi_2-\phi_1}{R_{\text{sheet}}} \end{aligned} \tag{12a}$$

where the unit vector $\boldsymbol{t}$ is tangential to the path, $\boldsymbol{n}_z\times\boldsymbol{n}=\boldsymbol{t}$, $\boldsymbol{J}_0=\boldsymbol{E}_0/\rho$, $\boldsymbol{E}_0=-\nabla\phi$, and $R_{\text{sheet}}=\rho/t_H$. Thus, the loop current is finite as long as the potentials are finite, but it may grow unboundedly if points 1 or 2 are singularities of the potential (e.g. if we force current through the device while the input contact becomes point sized and identical to point 1 or 2. This is similar to **Figure 7** in **Appendix A**). With the equivalent resistor network, it holds:

$$\phi_2-\phi_1=f\left(R_{ij}\right)I_{\text{supply}}=\frac{f\left(R_{ij,0}\right)}{\cos^2\theta_H}I_{\text{supply}} \tag{12b}$$

whereby $f\left(R_{ij}\right)$ is a ratio of polynomials in resistances of the equivalent resistor network. It has the dimension of a resistance. Points 1 and 2 can be inside the conductive region or on the boundary electrodes while the supply current can be injected via the same or via other electrodes. Combining (12a, b) gives:

$$\frac{I_{\text{loop},12}}{I_{\text{supply}}}=\frac{f\left(R_{ij,0}\right)}{R_{\text{sheet}}}\tan\theta_H \tag{12c}$$

Hence, the loop current can be smaller or larger than the supply current and it grows unboundedly for large Hall angle $\theta_H \to \pm 90^\circ$. For points 1 and 2 being on electrodes we can compute the loop current without knowledge of the geometry or topology, if we only know the equivalent resistor circuit. In **Figure 1(e)** for 1 A supply current the circulating current between both supply contacts divided by $\tan\theta_H = 10$ is equal to the supply voltage $\phi_{2,0} - \phi_{1,0} = 4.6886\ \mathrm{V}$ at zero applied magnetic field divided by the sheet resistance $I_{\mathrm{loop},12} / \tan\theta_H = \left(\phi_{2,0} - \phi_{1,0}\right) / R_{\mathrm{sheet}}$ (for $R_{\mathrm{sheet}} = 1\,\Omega$).

(12c) is essentially identical to (7) in [2], however, Green expressed the loop current in terms of the capacitance matrix of the electrode configuration instead of its resistance matrix $R_{ij,0}$.

The expression in (12c) is equal to the number of spiral loops of a current streamline within an annular region bordered by equipotential lines through points 1 and 2 (see also (B6a)).

4. Hall Plates with Point Current Contacts on Different Boundaries or in Their Interior

In **Figure 9** of part I [1], we studied the current pattern and the Hall potential in a rectangular sample with three holes—being square, oval, and triangular—where all boundaries were insulating and both current contacts were on the boundary of the large oval hole. There we noted no current spirals and the current pattern was constant versus applied magnetic field. The Hall voltage between points on the square and on the triangular hole vanished due to the specific locations of these holes. Now we revisit this triply connected Hall plate with insulating boundaries, yet this time we place one point current contact on the boundary of the square hole and the other point current contact on the boundary of the triangular hole. The current pattern changes dramatically: **Figure 2** shows massive spirals around both holes with current contacts—admittedly this happens only at huge applied magnetic field $\mu_H B_{a,z} = 30$ (88.1˚ Hall angle). Moreover, in contrast to part I, the current streamlines are not independent of the applied magnetic field any more: compare the different streamlines in **Figure 2(a)** & **Figure 2(b)** for positive and negative applied magnetic field. However, due to the principle of RMFR ([5] [6] [7]) there is no Hall voltage between points 2 and 3, which formerly were current contacts in **Figure 9** of part I. This holds for arbitrary applied magnetic field irrespective of the strength of the spirals (a proof is given in **Appendix C**). It also holds, if we move the current contacts arbitrarily along the boundaries of their respective holes (because in part I the Hall potential was homogeneous on all hole boundaries).

If we shrink all holes with single current contacts on their boundaries we end up with a Hall plate where current is supplied at interior points. These arrangements act similar to multiply connected Hall plates even though they might be simply connected. As an example **Figure 3** shows a circular disk where the current is injected in the center point and extracted at the rightmost point.

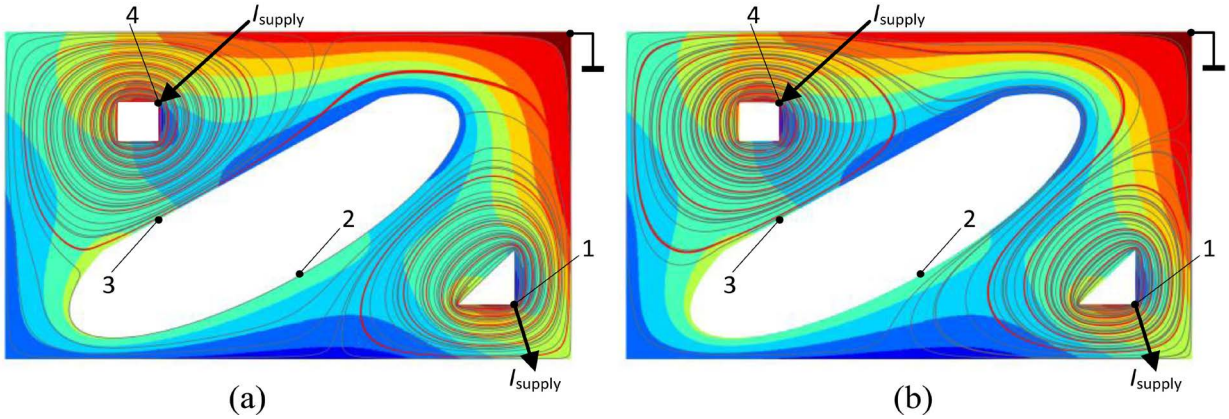

Figure 2. The same Hall plate with insulating boundaries as in **Figure 9** of part I [1], but here the point-sized current contacts are at boundaries of different holes: Current is input at point 4 on the boundary of the square hole and sunk at point 1 on the boundary of the triangular hole. A point on the perimeter is grounded, but no current flows into this ground node. Both figures show current streamlines in grey color and Hall potential according to the color map (red means 0 V, blue means −30 V): (a) for huge positive magnetic field $\mu_H B_{a,z} = 30$, (b) for huge negative magnetic field $\mu_H B_{a,z} = -30$. The Hall voltage between points 2 and 3—which were current inputs in **Figure 9** of part I—vanishes in spite of the complicated spiral current pattern. The Hall potential along all hole boundaries is not constant. Also, the Hall potential is not constant along the current streamlines. Two arbitrary streamlines are shown in red to guide the eye. They swirl in opposite directions around the current source and their sense of direction also changes with the sign of the Hall angle. All displayed quantities were obtained in FEM simulations with COMSOL MULTIPHYSICS in a plane conduction model with (1).

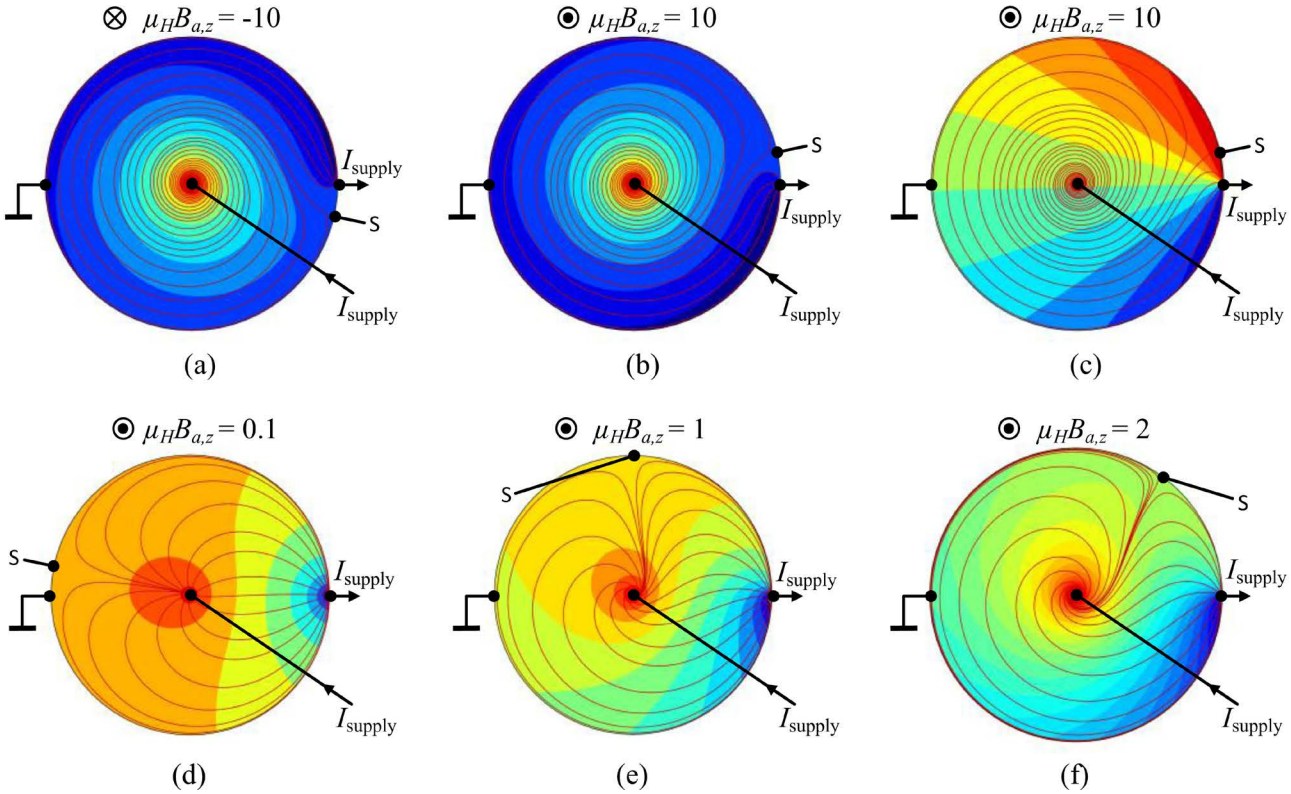

Figure 3. Circular Hall disk with current input in the center point and current output at the rightmost point. The leftmost point is grounded. Results are of 2D FEM simulations with COMSOL MULTIPHYSICS. All figures show current streamlines in red with the stagnation point labelled "S". The color-coding gives the electric potential in Figures (a), (b), (d), (e), (f) and the Hall potential in (c) (blue means negative, red positive values).

The leftmost point is grounded. This is similar to a Corbino disk but with point-sized instead of extended contacts. The analytical calculation is done in **Appendix A**. The figure shows the current streamlines, the potential, and the Hall potential at various magnetic fields as obtained by FEM simulations. Obviously, the Hall potential in **Figure 3(c)** is not constant along the current streamlines and the current streamlines are not constant versus applied magnetic field (compare **Figures 3(d)-(f)**). The current spiral around the inner current contact is infinitely strong with an infinite circulating current around the point current contact even at very small applied magnetic field (cf. **Appendix A**).

How can we explain this new phenomenon of spiral current patterns and the fact that current streamlines change with applied magnetic field in contrast to our findings in part I? Apparently, it has something to do with internal current sources. However, there are no spirals if current input and output are on the boundary of the same hole as in **Figure 9** of part I. On the other hand, the case of **Figure 3** can be regarded as a single point current contact on a hole boundary in the limit of vanishing hole size. Thus the communality is that *spiral current patterns are a product of internal hole boundaries being current sources or sinks*.

In the case of non-zero net current through a hole boundary it is obvious that the stream function ψ has a problem, because in **Section 5** of part I, we saw that ψ is constant on insulating boundaries between contacts, and it jumps across a contact by the amount of current through the contact (see (18) in part I). If the net current through all contacts on this boundary differs from zero the stream function faces a dilemma: it is forced to change also somewhere in-between two contacts. So the entire concept of a stream function crumbles.

Let us recall from part I that the stream function is proportional to the vertical magnetic field H_z caused by the currents J_x, J_y in an infinitely thick Hall plate with $\partial/\partial z = 0$. However, a stationary magnetic field due to a current makes sense only when this current flows in a closed loop. If the loop is opened, we will have $\nabla \cdot \boldsymbol{J} \neq 0$ at its ends and this violates Maxwell's first law $\nabla \times \boldsymbol{H} = \boldsymbol{J}$ because $\nabla \cdot \nabla \times \boldsymbol{H} = 0$. This is explained in [10] and it seems to address our problem particularly well. In **Figure 9(a)** of part I, we were inexact, because we did not show the full current loop, *i.e.*, how the current flows from a battery to the current input contact and from the current output contact back to the battery. Yet it is simple to add some curve through the big hole and insert a battery along this path (see **Figure 9(b)** of part I). Then the H_z field will have the same value within the hole at the RHS of this curve as it has on the right segment of the hole boundary. Also left of this curve the value of H_z will be identical to the one on the left segment of the hole boundary (see the blue and red hatched portions of the hole in **Figure 9(b)** of part I). H_z is discontinuous on infinitely many points, namely across the current return path. Luckily, these points are outside the conductive region. In these points H_z jumps by I_{supply}/t_H. Left and right of the current return path H_z must be constant because the thickness of the Hall plate is infinite (according to our 2D assumption

$\partial/\partial z = 0$) and there are no currents flowing inside the hole region except along the arbitrary current return path. Also in Figure 6 and Figure 7 of part I, we can close the current loops—there they can be closed *outside* the perimeter of the conductive regions. Therefore they add constant H_z outside the conductive regions. Hence, we did not miss these return paths when we discussed the stream function *inside* the conductive region. Finally, apart from the current return path—ψ is constant outside the conductive regions and inside the holes, and this agrees with the familiar notion $\boldsymbol{J} = \boldsymbol{0}$ there. In fact, this is even a simple explanation why ψ is constant on a hole boundary without current contacts: it is constant there because inside the entire hole $H_z = \text{constant}$ because no current flows inside the hole region.

The situation is different in Figure 2 and Figure 3. There we cannot close the current loop without cutting through the conductive region. We cannot solve this problem by pulling current straps out of the (*x*, *y*) drawing plane because the Hall plates are supposed to be infinitely thick for our H_z versus ψ analogy in part I [1], we are not allowed to work with 3D tricks in a 2D world. Hence, the return current path goes right through the conductive region and this will affect H_z and ψ there, too. Such a return current sheet will make H_z discontinuous at infinitely many points in the conductive region.

On the other hand, ignoring the current return path altogether gives wrong results for H_z and ψ, as the following example illustrates. Suppose an infinitely long hollow cylinder along z-direction. The cylinder consists of poorly conducting material like most high mobility semiconductors. No magnetic field is applied. The cylinder bore is clad with a perfectly conducting contact and also the outer surface is clad with the same material. If we tie one contact to ground and apply a voltage to the other contact a radial current density will result $\boldsymbol{J} \propto r^{-1}\boldsymbol{n}_r$. This is an infinitely thick Corbino disk at zero applied magnetic fields. What is the magnetic field generated by the current density? Solving Maxwell's first equation $\nabla \times \boldsymbol{H} = \boldsymbol{J}$ gives $\boldsymbol{H} = \boldsymbol{n}_z \arctan(y/x)$, but also $\boldsymbol{H} = -\boldsymbol{n}_z \arctan(x/y)$ is a solution. Thus, the solutions are discontinuous on x- and y-axes, respectively, and the solution is not even unique. Moreover, from physical intuition, we can consider a thin circular disk with radial current density. It will have only azimuthal magnetic field: CW above its top surface and CCW below its bottom surface. If we pile up an identical second circular disk the azimuthal fields of both disks cancel at their interface. Piling up infinitely many of them will cancel out the field in all test points. In the end, there is no (!) magnetic field caused by this current distribution—which of course contradicts Maxwell's first equation $\nabla \times \boldsymbol{H} = \boldsymbol{J}$ (current must always be accompanied by a magnetic field). What went wrong? The current loop was not closed. In reality, currents need to flow in both contacts parallel to the cylinder axis. Both currents vary versus *z*. The current on the inner contact generates an azimuthal magnetic field on its own within the conductive region. This cannot be handled in a 2D model. A complete 3D model must account for the vertical current component (see [11] [12]).

To sum up, *there exists no stream function, if the electrodes in a 2D conduction problem are placed in such a manner that the current return path via the battery cuts through the conductive region*. If both supply contacts are on the same boundary we can add a current return path outside the conductive region or inside a hole. Then the current density is equal to the curl of a unique magnetic field perpendicular to the plane of conduction. This is the stream function. It is continuous in nearly all points, *i.e.*, in all points with exception of a finite number of points (namely a finite number of point supply contacts on the boundaries). Then we can interpret ψ as a current potential function. Conversely, problems like in **Figure 2** and **Figure 3** have internal current sources, *i.e.*, single supply contacts on boundaries or within the conductive region. For them, we cannot close the current loop outside the conductive region or inside a hole in a 2D analysis. These current patterns are not identical to the curl of a unique vertical magnetic field.

In order to reconcile $\nabla\cdot\boldsymbol{J}\neq 0$ with Maxwell's first law $\nabla\times\boldsymbol{H}=\boldsymbol{J}$ we may add an extra current density $\boldsymbol{J}_e$ (*inside* the Hall effect region, not *outside*) which closes the current loop. From Maxwell, we know that every closed current loop is accompanied by a magnetic field $\boldsymbol{H}$, whereby the current density is the curl of $\boldsymbol{H}$.

$$\nabla\times\boldsymbol{H}=\boldsymbol{J}+\boldsymbol{J}_e \quad\Rightarrow\quad \nabla\cdot\boldsymbol{J}=-\nabla\cdot\boldsymbol{J}_e \tag{13}$$

Note that $\boldsymbol{J}_e$ may be a continuous function (as below in (14a)) or a discontinuous current return sheet (as in **Figure 7(b)** and **Figure 9(b)**, both in part I [1]). In both cases, the H_z-component has the physical meaning of a magnetic field generated by $\boldsymbol{J}+\boldsymbol{J}_e$ and with (11) in part I the stream function also specifies $\boldsymbol{J}+\boldsymbol{J}_e$ via $\boldsymbol{J}+\boldsymbol{J}_e=-\rho^{-1}\nabla\times\psi\boldsymbol{n}_z$. Of course, this procedure helps us only in the calculation of the current pattern $\boldsymbol{J}+\boldsymbol{J}_e$ and not for the original $\boldsymbol{J}$. But if $\boldsymbol{J}_e$ is known a priori, we can simply subtract it from $\boldsymbol{J}+\boldsymbol{J}_e$ to get $\boldsymbol{J}$. In the following, we will use $\boldsymbol{J}_e$ which is not known a priori, but which has a certain relation to $\boldsymbol{J}$. This will help us to break up the original problem into smaller sub-problems by decomposition of $\boldsymbol{J}$ into $\boldsymbol{J}_{\text{even}}$ and $\boldsymbol{J}_{\text{odd}}$.

If we choose $\boldsymbol{J}_e=-\boldsymbol{J}(-\boldsymbol{B}_a)$, contacts connected to current sources are no sources for the $\boldsymbol{J}+\boldsymbol{J}_e$ vector field, although they are sources for the $\boldsymbol{J}$ vector field. Therefore we may write according to (8) in part I and with $\boldsymbol{J}+\boldsymbol{J}_e=2\boldsymbol{J}_{odd}$.

$$\oint_C \boldsymbol{J}_{\text{odd}}\cdot\boldsymbol{n}\mathrm{d}s=0 \quad\Rightarrow\quad \boldsymbol{J}_{\text{odd}}=\nabla\times H_{z,\text{odd}}\boldsymbol{n}_z \tag{14a}$$

The meaning of (14a) is: Since $\boldsymbol{J}_{\text{odd}}$ is a vector field free of sources, its flux through any closed contour C in the multiply-connected Hall plate vanishes, and therefore $\boldsymbol{J}_{\text{odd}}$ can be expressed as the curl of a magnetic field $H_{z,\text{odd}}\boldsymbol{n}_z$. The label $H_{z,\text{odd}}$ is used to discriminate it against H_z in part I [1]. (14a) holds for Hall plates with both point-sized and extended contacts. With (14a) we can define a so-called *loop* stream function ψ_{loop} analogous to the conventional stream function ψ of part I.

$$\psi_{\text{loop}}=-\rho H_{z,\text{odd}} \tag{14b}$$

Analogous to part I, ψ_{loop} is constant along the streamlines of $\boldsymbol{J}_{\text{odd}}$, and therefore $\boldsymbol{J}_{\text{odd}} \cdot \nabla \psi_{\text{loop}} = 0$. Without internal current sources—like in part I—ψ_{loop} vanishes because then the current density is independent of the applied magnetic field: $\boldsymbol{J}(-\boldsymbol{B}) = \boldsymbol{J}(\boldsymbol{B}) \Rightarrow \boldsymbol{J}_{\text{odd}} = 0$. The definition implies that ψ_{loop} is an odd function of the applied magnetic field. Hence, ψ_{loop} depends on $\boldsymbol{B}_a$ whereas ψ in part I was constant w.r.t. $\boldsymbol{B}_a$. $\boldsymbol{J}_{\text{odd}}$ is linked to $\boldsymbol{H}_{\text{odd}}$ via (14a) and therefore $\nabla \times \boldsymbol{J}_{\text{odd}} = \boldsymbol{0}$. Hence ψ_{loop} fullfills the Laplace equation and it is constant on all boundaries *without* current contacts, because there is always a $\boldsymbol{J}_{\text{odd}}$-streamline that flows along such a boundary. If we insert (1) into (3c), we get with (2a-c) and (14a, b):

$$\nabla \phi_H = -\boldsymbol{n}_z \times \left[\mu_H B_{a,z} \nabla \phi_{\text{even}} + \left(1 + \mu_H^2 B_{a,z}^2\right) \nabla \psi_{\text{loop}} \right] \tag{15a}$$

These are the Cauchy-Riemann differential equations. It means that the function

$$F_{R,H} = -iF_{I,H} = \phi_H + i\left[\mu_H B_{a,z} \phi_{\text{even}} + \left(1 + \mu_H^2 B_{a,z}^2\right) \psi_{\text{loop}} \right] \tag{15b}$$

is analytical. We call it the complex Hall potential $F_{R,H}$ because its real part is the Hall potential ϕ_H, whereas the complex potential F_R in (21) of part I has the potential ϕ as its real part. (15b) differs from $F_{R,\text{odd}}$ in (22) of part I only in the term with the loop stream function. Therefore (15b) is a generalization of (22) in part I, because ψ_{loop} was zero there. Hence, both $F_{R,H}$ and $F_{R,\text{odd}}$ are odd in $B_{a,z}$. (15a) is equivalent to

$$\boldsymbol{n}_z \times \nabla \phi_H = \mu_H B_{a,z} \nabla \phi_{\text{even}} + \left(1 + \mu_H^2 B_{a,z}^2\right) \nabla \psi_{\text{loop}}. \tag{15c}$$

If we integrate the odd current density $\boldsymbol{J}_{odd}$ traversing a contour (extruded into thickness direction) that starts at point 1 and ends at point 2 we get with (14a, b).

$$\begin{aligned} I_{\text{loop},12} &= t_H \int_1^2 \boldsymbol{J}_{\text{odd}} \cdot \boldsymbol{n} \mathrm{d}s = \frac{t_H}{\rho} \int_1^2 \mathrm{d}s \boldsymbol{n} \cdot \boldsymbol{n}_z \times \nabla \psi_{\text{loop}} \\ &= \frac{-1}{R_{\text{sheet}}} \int_1^2 \mathrm{d}s \boldsymbol{t} \cdot \nabla \psi_{\text{loop}} = \frac{\psi_{\text{loop},1} - \psi_{\text{loop},2}}{R_{\text{sheet}}} \end{aligned} \tag{16}$$

If points 1 and 2 are left and right of a point current contact on a boundary, it holds $\int_1^2 \boldsymbol{J}(\boldsymbol{B}_a) \cdot \boldsymbol{n} \mathrm{d}s = \int_1^2 \boldsymbol{J}(-\boldsymbol{B}_a) \cdot \boldsymbol{n} \mathrm{d}s$. Inserting this into (16) shows that ψ_{loop} is also continuous on boundaries *with* point current contacts, whereas in part I ψ was discontinuous there. On extended contacts ψ_{loop} has identical values at both ends, but it varies along the contact. If points 1 and 2 in (16) are point supply contacts on different boundaries, $I_{\text{loop},12}$ is the total circulating current that flows in the Hall plate. It can be smaller or larger than the supply current and it can even become infinite (see **Appendix A**). In the absence of internal current sources, *i.e.*, when both point supply contacts are on the same boundary, the circulating current vanishes, because then the loop stream function vanishes. If we use Maxwell's law in the quasistatic case $\oint \boldsymbol{E} \cdot \mathrm{d}\boldsymbol{s} = 0$ at positive and negative applied magnetic field and subtract both equations it gives $\oint \boldsymbol{E}_H \cdot \mathrm{d}\boldsymbol{s} = 0$ (see (3c)). Inserting (1) gives the circulation Γ of the odd current density $\boldsymbol{J}_{\text{odd}}$ if the curve C encircles the current input contact.

$$\Gamma = \oint_C \boldsymbol{J}_{\text{odd}} \cdot \mathrm{d}\boldsymbol{s} = \mu_H B_{a,z} \oint_C \boldsymbol{J}_{\text{even}} \cdot \boldsymbol{n}\mathrm{d}s$$
$$= \mu_H B_{a,z} \oint_C \left(\boldsymbol{J}_{\text{even}} + \boldsymbol{J}_{\text{odd}}\right) \cdot \boldsymbol{n}\mathrm{d}s = \mu_H B_{a,z} \frac{I_{\text{supply}}}{t_H} \tag{17a}$$

In (17a), we were allowed to add $\boldsymbol{J}_{\text{odd}}$ in the integrand because integration of $\boldsymbol{J}_{\text{odd}} \cdot \boldsymbol{n}$ over a closed path gives zero according to (16). The circulation of a specific pattern of spiral current streamlines is computed in **Appendix A**. Note that the circulation in (17a) is identical to the circulation in Hall plates where all boundaries are contacts (see (11c)). On the other hand, if we use $\oint \boldsymbol{E}_{\text{even}} \cdot \mathrm{d}\boldsymbol{s} = 0$ and (1) and (14a, b) it follows:

$$\oint_C \boldsymbol{J}_{\text{even}} \cdot \mathrm{d}\boldsymbol{s} = 0 \tag{17b}$$

With $\boldsymbol{J} = \boldsymbol{J}_{\text{even}} + \boldsymbol{J}_{\text{odd}}$ and (17a, b), it is clear that the circulation of $\boldsymbol{J}$ is equal to the circulation of $\boldsymbol{J}_{\text{odd}}$. Spiral current streamlines appear only for $\boldsymbol{J}_{\text{odd}} \neq \boldsymbol{0}$. Therefore we have no spirals in the absence of internal current sources like in part I [1], where it holds $\boldsymbol{J}_{\text{odd}} = \boldsymbol{0}$ (because $\boldsymbol{J}$ was independent of $\boldsymbol{B}_a$). Conversely, in the case of internal current sources there are also no spirals at $\boldsymbol{B}_a = \boldsymbol{0}$. Thus, it needs applied magnetic field *and* internal current sources to produce circulating current. Thereby it is irrelevant if the internal current sources are embedded in the conductive region or if they are on boundaries of holes in the conductive region. The method of Corbino images from [13] is also a way to prove that the circulation around single point contacts is given by (17a) and that it vanishes when both supply contacts are encircled. In [13] this method was used for conductive regions with one boundary, but it can also be generalized for more boundaries (like ring domains) if one uses a superposition of infinitely many images [14] [15].

Inserting the right hand sides of (3b, c) into (6d) and eliminating the vector product by use of (15c) gives:

$$\boldsymbol{J}_{\text{even}} = \frac{-1}{\rho} \nabla \left(\phi_{\text{even}} + \mu_H B_{a,z} \psi_{\text{loop}}\right) \tag{18}$$

In (18), the terms in the brackets act like a potential, which fulfills the Laplace equation because of $\nabla^2 \phi_{\text{even}} = 0$ and $\nabla^2 \psi_{\text{loop}} = 0$. On the boundary $\boldsymbol{J}_{\text{even}} \cdot \boldsymbol{n}$ is given – it is zero at the insulating boundary and it is a Dirac delta pulse of strength $\pm I_{\text{supply}} / t_H$ at the point-sized supply contacts. However, $-\rho \boldsymbol{J}_{\text{even}} \cdot \boldsymbol{n}$ is the normal derivative of the bracket term in (18), which is a von Neumann boundary condition that does not depend on the applied magnetic field. Therefore the term in the brackets of (18) does not depend on the applied magnetic field. Yet, at $B_{a,z} = 0$ it is equal to ϕ_0 (up to an arbitrary additive constant) and therefore

$$\phi_0 = \phi_{\text{even}} + \mu_H B_{a,z} \psi_{\text{loop}}. \tag{19}$$

In (19), we implicitly assume the arbitrary additive constant in ψ_{loop} such that $\psi_{\text{loop}} = 0$ in the ground node where it holds $\phi_0 = \phi_{\text{even}} = 0$. On the other hand, we want to interprete $-\psi_{\text{loop}} / \rho$ as the magnetic field $H_{z,\text{odd}}$ caused by

$\boldsymbol{J}_{\text{odd}}$. Since $\boldsymbol{J}_{\text{odd}}$ vanishes outside the perimeter of the Hall plate, also $H_{z,\text{odd}}=0$ there. Therefore *we have to ground a point on the perimeter of the multiply-connected Hall plate*.

(19) in (18) with $\boldsymbol{E}_0/\rho=\boldsymbol{J}_0$ gives:

$$\boldsymbol{J}_{\text{even}}=\boldsymbol{J}_0 \tag{20}$$

which is identical to (10a) in **Section 3** (both times the Hall plates are supplied by constant current sources). (19) can be seen as an alternative definition of the loop stream function, being the negative increase in even potential divided by $\mu_H B_{a,z}$. Since ψ_{loop} does not change along any hole or perimeter boundaries, $\phi_{\text{even}}-\phi_0$ is also homogeneous there according to (19). With (19) we can eliminate the even potential in (15b).

$$F_{R,H}=-iF_{I,H}=\phi_H+i\left(\mu_H B_{a,z}\phi_0+\psi_{\text{loop}}\right) \tag{21a}$$

$$\nabla\phi_H=-\boldsymbol{n}_z\times\left(\mu_H B_{a,z}\nabla\phi_0+\nabla\psi_{\text{loop}}\right) \tag{21b}$$

Curves of constant Hall potential are orthogonal to curves of constant $\mu_H B_{a,z}\phi_0+\psi_{\text{loop}}$.

Next, we compute the Hall electric field perpendicular to an insulating boundary from (6a) with $\boldsymbol{J}_{\text{odd}}\cdot\boldsymbol{n}=0$ and with (20).

$$\boldsymbol{E}_H\cdot\boldsymbol{n}=-\boldsymbol{n}\cdot\nabla\phi_H=\frac{-\partial\phi_H}{\partial n}=\rho\mu_H B_{a,z}\boldsymbol{J}_0\times\boldsymbol{n}_z\cdot\boldsymbol{n}=\rho\mu_H B_{a,z}\boldsymbol{J}_0\cdot\boldsymbol{t} \tag{22}$$

Thus, the Hall potential is a harmonic function, which satisfies von Neumann boundary conditions with values that are linearly proportional to applied magnetic field. Therefore ϕ_H is perfectly linear in $\mu_H B_{a,z}$ (the same applies to Hall plates with insulating boundaries and point-sized contacts *without* internal current sources, see part I [1]). With (21a, b) it follows that ψ_{loop} is also perfectly linear in $\mu_H B_{a,z}$. Therefore, also $\boldsymbol{J}_{odd}$ is linear in $\mu_H B_{a,z}$ (see (14a,b)). Consequently, the total current pattern $\boldsymbol{J}=\boldsymbol{J}_0+\boldsymbol{J}_{odd}$ is *not* constant versus applied magnetic field – which is in contrast to the Hall plates discussed in part I. Therefore, *in the case of internal current sources the current density depends on the applied magnetic field even if the contacts are only point-sized*. This explains the different streamlines at positive and negative magnetic field in **Figure 2(a)** & **Figure 2(b)**. At positive Hall angle they go counter-clockwise (CCW) around the current input at the square hole and clockwise (CW) around the current sink at the triangle. At negative Hall angle the directions of the spirals are inverted.

From (19) it follows that $\phi_{\text{even}}-\phi_0$ is proportional to the second power of $\mu_H B_{a,z}$. In other words, $\left(\phi_{\text{even}}-\phi_0\right)/\left(\mu_H B_{a,z}\right)^2$ does not depend on the applied magnetic field, and since it is equal to $\psi_{\text{loop}}/\left(\mu_H B_{a,z}\right)$ it is constant on all boundaries. Moreover, $\left(\phi_{\text{even}}-\phi_0\right)/\left(\mu_H B_{a,z}\right)^2$ is a solution of the Laplace equation. Consequently, $\psi_{\text{loop}}/\left(\mu_H B_{a,z}\right)$ is linearly proportional to the potential $\tilde{\phi}_0$ of the very same Hall plate with the same supply current into the same supply current contacts but all boundaries are conducting (like in **Section 3**) instead of insulating.

$$\psi_{\text{loop}}=c_1\mu_H B_{a,z}\tilde{\phi}_0 \tag{23a}$$

In (23a), we chose the arbitrary additive constant of $\tilde{\phi}_0$ being a solution of the Laplace equation such that $\tilde{\phi}_0 = 0$ where $\psi_{\text{loop}} = 0$, *i.e.*, the electrode being the perimeter must be grounded. The constant c_1 follows from the circulation. Inserting (23a) into (17a) gives:

$$\begin{aligned}\Gamma &= \oint_C \boldsymbol{J}_{\text{odd}} \cdot \mathrm{d}\boldsymbol{s} = c_1 \mu_H B_{a,z} \oint_C \mathrm{d}s \boldsymbol{n} \cdot \frac{\nabla \tilde{\phi}_0}{\rho} \\ &= -c_1 \tan\theta_H \oint_C \tilde{\boldsymbol{J}}_0 \cdot \boldsymbol{n} \mathrm{d}s = -c_1 \tan\theta_H \frac{I_{\text{supply}}}{\mathrm{t_H}}\end{aligned} \tag{23b}$$

Setting this equal to (11c) gives:

$$c_1 = -1 \tag{23c}$$

(23a, c) relate the loop stream function in a multiply-connected Hall plate with insulating boundaries to the potential at zero applied magnetic field in the same Hall effect region, yet with all boundaries being electrodes. Therefore, on the contacts ψ_{loop} is a function of the resistors $R_{ij,0}$ of **Section 3**. We do not even need to know the geometry of the Hall plate to compute it—it already follows from the equivalent resistor circuit $R_{ij,0}$ at zero applied magnetic field for the Hall plate with all boundaries being contacts. Inserting (23a) into (16) with points 1 and 2 being negative and positive supply contacts, respectively, and comparing to (12c) proves that the total circulating current is identical in two identical Hall regions with (i) point sized contacts with insulating boundaries and (ii) all boundaries conducting, provided the same supply current is injected.

Inserting (23a) into (21a) gives:

$$F_{R,H} = -iF_{I,H} = \phi_H + i\mu_H B_{a,z}\left(\phi_0 - \tilde{\phi}_0\right) \tag{24}$$

Thus, the lines of constant Hall potential are orthogonal to the lines of constant $\phi_0 - \tilde{\phi}_0$. Therefore, the Hall voltage vanishes, if it is sampled between two points on the same streamline of the current vector field $\boldsymbol{J}_0 - \tilde{\boldsymbol{J}}_0$, whereby $\boldsymbol{J}_0$ is the current density of the Hall plate with all boundaries being insulating and $\tilde{\boldsymbol{J}}_0$ is the current density of the Hall plate with all boundaries being electrodes, and both Hall plates are supplied with the same fixed current at zero applied magnetic field.

Inserting (23a, c) into (14a, b) shows that at fixed supply current the odd current density in the Hall plate with insulating boundaries is identical to the odd current density in the same Hall effect region with all boundaries being electrodes.

$$\boldsymbol{J}_{odd} = \tilde{\boldsymbol{J}}_{odd} = \tan\theta_H \boldsymbol{n}_z \times \tilde{\boldsymbol{J}}_0 \tag{25}$$

With (20) and (25) we can express even and odd current densities and electric fields via $\boldsymbol{J}_0$ and $\tilde{\boldsymbol{J}}_0$, so that from now on we would not need ψ_{loop} any more.

$$\boldsymbol{E}_H = \rho \tan\theta_H \left(\boldsymbol{J}_0 - \tilde{\boldsymbol{J}}_0\right) \times \boldsymbol{n}_z \tag{26}$$

Integrating the Hall electric field along a path from point 1 to point 2 gives with (26):

$$\begin{aligned}\int_1^2 \boldsymbol{E}_H \cdot \mathrm{d}\boldsymbol{s} &= -\int_1^2 \mathrm{d}s\ \boldsymbol{t}\cdot\nabla\phi_H = -\int_1^2 \mathrm{d}\phi_H = \phi_{H,1}-\phi_{H,2}\\ &= \rho\tan\theta_H \int_1^2 \mathrm{d}s\ \boldsymbol{t}\cdot\left(\boldsymbol{J}_0-\tilde{\boldsymbol{J}}_0\right)\times\boldsymbol{n}_z\\ &= \rho\tan\theta_H \int_1^2 \mathrm{d}s\left(\tilde{\boldsymbol{J}}_0-\boldsymbol{J}_0\right)\cdot\boldsymbol{n}\\ &= R_{\text{sheet}}\tan\theta_H\left(\tilde{I}_{0,12}-I_{0,12}\right)\end{aligned} \tag{27a}$$

where $\tilde{I}_{0,12}, I_{0,12}$ are the currents flowing across a contour that connects points 1 and 2. Thereby the applied magnetic field vanishes and all boundaries of the Hall plate are electrodes (for $\tilde{I}_{0,12}$) and insulating (for $I_{0,12}$), respectively. Thereby the same supply current flows into the same boundaries. Analogous to (7) and (19) in Part I, we can write for the Hall voltage between arbitrary points 1 and 2

$$V_{H,12} = I_{\text{supply}} R_{\text{sheet}} G_{H,12} \tan\theta_H \tag{27b}$$

with the Hall geometry factor

$$G_{H,12} = \frac{\tilde{I}_{0,12}-I_{0,12}}{I_{\text{supply}}} \tag{27c}$$

Thus, the Hall geometry factor is again (like in part I) a ratio of a current flowing across a contour connecting the two point-sized output contacts over the supply current, however, here we have $\tilde{I}_{0,12}-I_{0,12}$ in the numerator, whereas we had $-I_{12}=-I_{0,12}$ in part I. Note that in part I point-sized current input and output contacts were at the same boundary, which means $\tilde{I}_{0,12}=0$, because the electrode on that boundary is a perfect short. Therefore, (27c) is a generalization of (19) in part I. If the points 1 and 2 are on the same boundary the current $\tilde{I}_{0,12}$ goes continuously to zero as the two points approach, whereas the current $I_{0,12}=I_{\text{supply}}$ if a supply contact is between points 1 and 2. This means that along boundaries the Hall voltage jumps abruptly across point current contacts and it varies smoothly on the rest of the boundary. Due to the subtraction in (27c) the Hall voltage along boundaries is smaller in the case of spiral current streamlines than in the absence of internal current sources like in part I. (27b, c) also show that locations of zero Hall voltage do no change versus applied magnetic field.

A comparison of this section with the preceding one shows that the Hall electric field in multiply connected Hall plates vanishes everywhere if all boundaries are highly conducting, whereas it is proportional to the applied magnetic field everywhere if all boundaries are insulating.

Figure 4 shows the spiral current streamlines and the loop stream function for the Hall plate of Figure 2 with the same current supply contacts: $\boldsymbol{J}_{\text{odd}}$ flows in closed loops around the current contacts while ψ_{loop} is constant on these loops. Thus ψ_{loop} is also constant on all hole boundaries and zero on the outer boundary, just as we would expect it for the vertical magnetic field $H_{z,\text{odd}}$ generated by a current vector field $\boldsymbol{J}_{\text{odd}}$ according to (14a). Figure 5 shows that $\phi_{\text{even}}-\phi_0$ is constant on all boundaries. Figure 6 shows that the streamlines of $\boldsymbol{J}_0-\tilde{\boldsymbol{J}}_0$ flow along equipotential lines of the Hall potential.

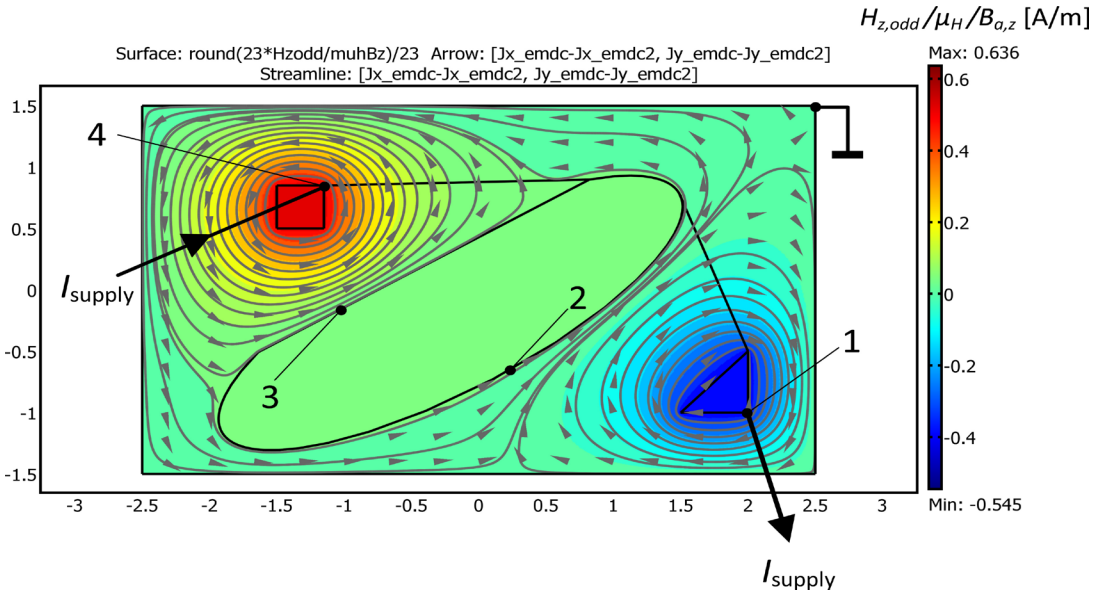

Figure 4. The same Hall plate with insulating boundaries as in **Figure 2**, with the same supply current of 1 A into the same point current contacts 4 and 1. The grey lines are streamlines of $\boldsymbol{J}_{odd}$. They are not spirals, but closed loops around the holes with the current contacts. The grey cones denote the orientation of $\boldsymbol{J}_{odd}$. The color-coding denotes the magnetic field $H_{z,odd}$ in A/m normalized by $\mu_H B_{a,z}$. All results are obtained by three coupled FEM calculations with COMSOL MULTIPHYSICS: two are conductive media calculations with the conductivity tensor from (1) for positive and negative applied magnetic field $\mu_H B_{a,z} = \pm 10$. The resulting current density for positive magnetic field is denoted by the components Jx_emdc, Jy_emdc. The result for negative magnetic field is Jx_emdc2, Jy_emdc2. Half the difference of current densities in these two calculations is set equal to $\boldsymbol{J}_{odd} = (\text{Jx\_emdc-Jx\_emdc2})\,\boldsymbol{n}_x/2 + (\text{Jy\_emdc-Jy\_emdc2})\,\boldsymbol{n}_y/2$. The third calculation computes the magnetic field $H_{z,odd}$ in response to $\boldsymbol{J}_{odd}$, whereby the boundary condition was "electric insulation" ($H_{z,odd} = 0$) on the outer boundary. The current streamlines are identical with the contour lines of $H_{z,odd}$. The hole boundaries are also contour lines of $H_{z,odd}$ with values of 6.36, 0.24, −5.45 A/m for the square hole, the large hole, and the triangular hole, respectively. Inside the holes the $H_{z,odd}$-field is homogeneous. No current flows into the ground node on the perimeter.

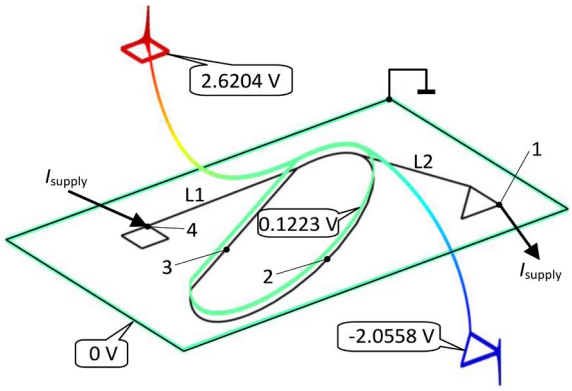

Figure 5. The same Hall plate with insulating boundaries as in **Figure 2** and **Figure 4**, with the same supply current of 1 A into the same point current contacts 4 and 1. The geometry is drawn in black lines. The color lines denote the function $-\psi_{loop} = (\phi_{even} - \phi_0)/(\mu_H B_{a,z})$ where blue means negative, green means zero, and red means positive (the precise values are given as labels). The height above/below the Hall plate also denotes $(\phi_{even} - \phi_0)/(\mu_H B_{a,z})$. Evidently, the hole boundaries and the perimeter boundary are at constant values. The spikes in the current contacts are due to insufficient meshing in these singular points. The two lines L1, L2 are virtual lines without physical meaning (compare **Figure 9(b)** in part I [1]). The results are obtained by three conductive media FEM calculations with COMSOL MULTIPHYSICS with the conductivity tensor from (1) for $\mu_H B_{a,z} = \pm 10$ and $\mu_H B_{a,z} = 0$.

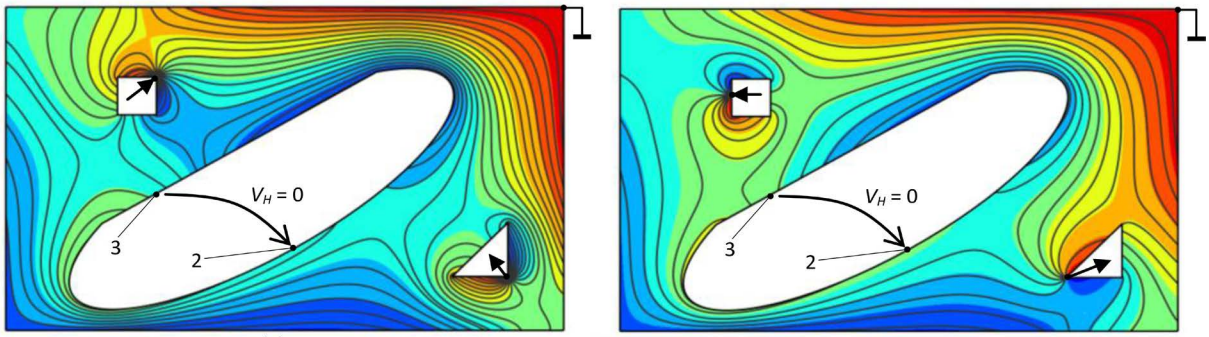

Figure 6. The same Hall plate with insulating boundaries as in **Figure 2**, **Figure 4** and **Figure 5**. The grey streamlines denote $\boldsymbol{J}_0 - \tilde{\boldsymbol{J}}_0$ and the color map gives the Hall potential at $\mu_H B_{a,z} = \pm 10$ (red means 0 V, blue means −10 V). (a), (b) different point current contacts on the same hole boundaries. The supply current is 1 A. The ground node is a point on the perimeter. No current flows into this ground node. Obviously, the streamlines are identical with equipotential lines of the Hall potential. The Hall voltage between points 2 and 3 vanishes due to RMFR, because they were current contacts in **Figure 9** of part I [1] while the boundaries of the square and triangular holes were on the same streamline of $\boldsymbol{J}$. Therefore, the color map has identical color at points 2 and 3. The results are obtained by four conductive media FEM calculations with COMSOL MULTIPHYSICS with the conductivity tensor from (1) for $\mu_H B_{a,z} = \pm 10$ and $\mu_H B_{a,z} = 0$ first with insulating boundaries and then with all boundaries being electrodes.

Finally, we briefly mention that there are alternative ways to tackle the problem of **Section 4**. Instead of the loop stream function, one could also define a generalized stream function Ψ with:

$$\boldsymbol{J}_0 - \tilde{\boldsymbol{J}}_0 = -\nabla \times \frac{\Psi}{\rho} \boldsymbol{n}_z \tag{28}$$

because $\oint \left(\boldsymbol{J}_0 - \tilde{\boldsymbol{J}}_0 \right) \cdot \boldsymbol{n} \mathrm{d}s = 0$ for all closed paths in a multiply-connected 2D Hall effect region (compare with (8) in part I). Inside the Hall effect region, it holds $\nabla \cdot \left(\boldsymbol{J}_0 - \tilde{\boldsymbol{J}}_0 \right) = -\rho^{-1} \left(\nabla^2 \phi_0 - \nabla^2 \tilde{\phi}_0 \right) = 0$. Ψ does not depend on the applied magnetic field. Then we get with (26):

$$\phi_H = -\tan \theta_H \Psi \tag{29}$$

where we define $\Psi = 0$ in the ground node. These equations have greater similarity to (13) and (17a) in part I.

5. A Summary of Simple Rules

In parts I and II, we derived simple rules to understand the classical (non-quantum) Hall potential in thin, plane and homogeneous regions with linear material properties. Here we compile them.

It turns out that internal current sources are a key issue in multiply-connected Hall plates. A plane two-dimensional current distribution is free of internal current sources if (i) there is no current flowing into or out of any interior point, and (ii) if the net current flowing into or out of any closed hole boundary or the perimeter boundary is zero. A stream function exists only in the absence of internal current sources. Conversely, spiral current streamlines originate only from internal current sources. However, in this latter case, at least the odd part

of the current density can be obtained from a loop stream function. Stream function and loop stream function can be interpreted as the vertical component of a magnetic field generated by the respective current in the Hall plate with infinite thickness.

Without internal current sources and when all boundaries are insulating (apart from point sized current contacts) the current density is constant versus changes in applied magnetic field. The Hall potential is constant along all current streamlines. Since any closed boundary (hole boundary or perimeter) without current contacts is encircled by a single current streamline, the Hall potential is constant on the boundary. Therefore, the Hall voltage between any two points on such a boundary vanishes. In all test points, the Hall potential is linearly proportional to $\mu_H B_{a,z}$. The Hall voltage between any two points is proportional to the current flowing across a contour between both points.

If there are no current sources in the Hall plate but at least one contact is extended, the current density changes versus applied magnetic field. Then, in general, the Hall voltage between two points on the same boundary does not vanish, even if that boundary has no current contacts. The Hall voltage is not strictly linear versus applied magnetic field. At very large Hall angles extended contacts become similar to point-sized contacts located at one of both ends of the extended contacts—which one depends on the polarity of the applied magnetic field. Therefore, at very large Hall angles the Hall voltage diminishes if it is tapped between points with no current flowing in-between (e.g. on hole boundaries with no contacts).

If the peripheral boundary and all hole boundaries of a multiply-connected Hall plate are electrodes there is no Hall voltage between any points (or contacts) of the Hall plate. The device acts like a network of resistors, whose resistances are proportional to $1+\mu_H^2 B_{a,z}^2$. This is the only case when a Hall plate is reciprocal instead of reverse magnetic field reciprocal.

If a Hall plate has internal current sources, the total current density changes versus applied magnetic field regardless of the size of the contacts. However, in the absence of extended contacts at least the even part of the current density is constant versus applied magnetic field, whereas the odd current density and the Hall potential are linear versus applied magnetic field. Then the odd current density is identical to the one in the same Hall plate, yet with all boundaries being electrodes. Therefore the circulation of the current density does not depend on the size of the electrodes. The Hall voltage vanishes between two points on the same streamlines of $\boldsymbol{J}_0 - \tilde{\boldsymbol{J}}_0$, *i.e.*, the difference in current densities at zero applied magnetic field with point contacts and with all boundaries being electrodes. Along boundaries, the Hall potential jumps across point-sized current contacts and if there are no current contacts it varies smoothly according to current density flowing through this boundary in case all boundaries were electrodes. If current enters or exits the Hall plate through a point in its interior the current streamlines encircle this point infinitely many times even at very weak

applied magnetic field and at very small supply current. Then there flows an infinite circulating current around this point. However, this applies only to points in a mathematical sense (infinitely small ones). Otherwise, if the net current into a hole boundary differs from zero, the current streamlines may encircle the hole zero times, once, or several (finite) times, depending on the strength of the applied magnetic field. The current streamlines swirl around internal current sources in CW or CCW direction, depending on the polarity of the current and of the applied magnetic field and on the sign of the charge carriers. In particular, positive and negative charge carriers swirl around a contact in opposite directions (at identical polarities of current and applied magnetic field). In current spirals, the self-field of the current adds to the applied magnetic field constructively if the positive or negative charge carriers flow into the spiral.

Table 1 gives a survey of the properties of the electric quantities of multiply-

Table 1. Overview of the properties of the electric quantities of thin, homogeneous, plane, multiply-connected Hall plates with constant supply current with boundaries being all insulating or all conducting at $\boldsymbol{B}_a = B_{a,z}\boldsymbol{n}_z$ with homogeneous $B_{a,z}$. Resistivity ρ and Hall mobility μ_H are constant versus $\boldsymbol{E}$ and $\boldsymbol{B}_a$.

Plane multiply-connected Hall plates with constant supply current		
All boundaries are insulating		All boundaries are conducting
Reverse Magnetic Field Reciprocity holds		Reciprocity holds
No internal current sources	Internal current sources	w/o internal current sources
$\boldsymbol{J}_{\text{even}} = \boldsymbol{J}_0$	$\boldsymbol{J}_{\text{even}} = \boldsymbol{J}_0$	$\tilde{\boldsymbol{J}}_{\text{even}} = \tilde{\boldsymbol{J}}_0$
$\boldsymbol{J}_{\text{odd}} = \boldsymbol{n}_z \times \nabla \psi_{\text{loop}} / \rho \Rightarrow \boldsymbol{J}_{\text{odd}} = \boldsymbol{0}$	$\boldsymbol{J}_{\text{odd}} = \tan\theta_H \boldsymbol{n}_z \times \tilde{\boldsymbol{J}}_0 = \tilde{\boldsymbol{J}}_{\text{odd}} \propto \tan\theta_H$	
$\psi_{loop} = 0$	$\boldsymbol{J}_{\text{odd}} = \boldsymbol{n}_z \times \nabla \psi_{\text{loop}} / \rho \Rightarrow \psi_{\text{loop}} = -\tan\theta_H \tilde{\phi}_0$	
$\boldsymbol{J} = \boldsymbol{J}_0 = \boldsymbol{n}_z \times \nabla \psi / \rho$ constant versus θ_H	$\boldsymbol{J} = \boldsymbol{J}_0 + \tan\theta_H \boldsymbol{n}_z \times \tilde{\boldsymbol{J}}_0$ changes with θ_H	$\tilde{\boldsymbol{J}} = \tilde{\boldsymbol{J}}_0 + \tan\theta_H \boldsymbol{n}_z \times \tilde{\boldsymbol{J}}_0$ changes with θ_H
$\boldsymbol{E}_{\text{even}} = \rho \boldsymbol{J}_0$	$\boldsymbol{E}_{\text{even}} = \rho \boldsymbol{J}_0 + \tan^2\theta_H \rho \tilde{\boldsymbol{J}}_0$	$\tilde{\boldsymbol{E}} = \tilde{\boldsymbol{E}}_{\text{even}} = \rho \tilde{\boldsymbol{J}}_0 / \cos^2\theta_H$
$\phi_{\text{even}} - \phi_0 = 0$	$\phi_{\text{even}} - \phi_0 = \tilde{\phi}_0 \tan^2\theta_H = \tilde{\phi}_{\text{even}} - \tilde{\phi}_0$	
$\boldsymbol{E}_H = \rho \tan\theta_H \boldsymbol{J}_0 \times \boldsymbol{n}_z \propto \tan\theta_H$	$\boldsymbol{E}_H = \rho \tan\theta_H \left(\boldsymbol{J}_0 - \tilde{\boldsymbol{J}}_0\right) \times \boldsymbol{n}_z \propto \tan\theta_H$	$\tilde{\boldsymbol{E}}_H = \boldsymbol{0}$
$\phi_H = -\psi \tan\theta_H \propto \tan\theta_H$	$\phi_H \propto \tan\theta_H$	$\tilde{\phi}_H = 0$
$G_{H,12} = \dfrac{-I_{12}}{I_{\text{supply}}}$ with $I_{12} = I_{12,0}$	$G_{H,12} = \dfrac{\tilde{I}_{0,12} - I_{0,12}}{I_{\text{supply}}}$	$G_{H,12} = 0$
ψ does not depend on θ_H	$\psi_{\text{loop}} \propto \tan\theta_H$	$\tilde{\phi}\cos^2\theta_H$ does not depend on θ_H
ϕ_H and ψ are homogeneous along boundaries without current contacts	$\phi_{\text{even}} - \phi_0$ and ψ_{loop} are homogeneous along all boundaries	$\tilde{\phi}$ is homogeneous along all contacts
ϕ_H is homogeneous on streamlines of $\boldsymbol{J}_0$	ϕ_H is homogeneous on streamlines of $\boldsymbol{J}_0 - \tilde{\boldsymbol{J}}_0$	$\tilde{\phi}_H = 0$ everywhere
$F_k = (1 + i\tan\theta_H)(\phi_0 + i\psi)$	$F_{k,H} = \phi_H + i\tan\theta_H \left(\phi_0 - \tilde{\phi}_0\right)$	-
$\Gamma = 0$ no current spirals	$\Gamma = \tan\theta_H I_{\text{supply}} / \text{t}_{\text{H}}$ current spirals	w/o current spirals

connected Hall plates with constant supply current. Medium-sized contacts are excluded.

6. Discussion

We found that the boundary conditions have a dominant impact on the electric potential in a multiply connected Hall region. The magnitude of the Hall potential at arbitrary points in the Hall plate depends on the percentage of the total boundary covered with electrodes. If all boundaries are electrodes, the Hall potential vanishes everywhere in the Hall effect region, *i.e.*, the Hall effect is inactive. Conversely, if all boundaries are insulating and the contacts are only point-sized, the Hall potential is strictly proportional to $\mu_H B_{a,z}$ everywhere in the Hall effect region. In both cases, the even current density is not affected by the applied magnetic field provided that the Hall plate is supplied with constant current.

A major portion of this work was devoted to multiply-connected Hall plates with insulating boundaries and point-sized contacts, for which we developed a new theory. In part I, we showed that the Hall voltage vanishes if it is tapped between two points on a boundary without current contacts. This is the case in Hall/Anti-Hall bars. In part II, we introduced internal current sources and then a Hall voltage between the very same taps exists again!

Our new theory can be applied to Hall plates with anisotropic conductivity as it is caused by mechanical stress in a cubic crystal. Then, in a preceding isotropization step, one can replace the original geometry by a distorted geometry with isotropic conductivity (see [16] and references therein). This procedure does not change the number of holes in a multiply-connected Hall plate. It also preserves point-sized contacts and boundaries, which are being entirely covered by electrodes. Therefore, we expect no new phenomena in multiply-connected Hall plates with anisotropic conductivity.

For engineering purposes, the magnitude of the Hall potential is less important than its ratio over noise at given impedance level and costs for chip area. Under these boundary conditions, Hall plates with peripheral medium sized contacts turn out to be optimum [17].

Acknowledgements

The author gratefully acknowledges the vivid and fruitful discussions with both Prof. Dieter Süss of University of Vienna (Austria) and Dr. William J. Bruno of New Mexico Consortium, Los Alamos, NM (USA).

Conflicts of Interest

The authors declare no conflicts of interest regarding this publication of this paper.

References

[1] Ausserlechner, U. (2019) The Classical Hall Effect in Multiply-Connected Plane Re-

gions Part I: Topologies with Stream Function. *Journal of Applied Mathematics and Physics*, **7**, 1968-1996. https://doi.org/10.4236/jamp.2019.79136

[2] Green, M. (1961) Electrode Geometries for Which the Transverse Magnetoresistance Is Equivalent to That of a Corbino Disk. *Solid-State Electronics*, **3**, 314-316. https://doi.org/10.1016/0038-1101(61)90014-4

[3] Haeusler, J. (1967) Die Untersuchung von Potentialproblemen bei tensorieller Leitfähigkeit der Halbleiter und Plasmen im transversalen Magnetfeld. Dissertation TH Stuttgart. (In German)

[4] Moelter, M.J., Evans, J., Elliott, G. and Jackson, M. (1998) Electric Potential in the Classical Hall Effect: An Unusual Boundary-Value Problem. *American Journal of Physics*, **66**, 668-677. https://doi.org/10.1119/1.18931

[5] Spal, R. (1980) A New DC Method of Measuring the Magnetoconductivity Tensor of Anisotropic Crystals. *Journal of Applied Physics*, **51**, 4221-4225. https://doi.org/10.1063/1.328281

[6] Sample, H.H., Bruno, W.J., Sample, S.B. and Sichel, E.K. (1987) Reverse-Field Reciprocity for Conducting Specimens in Magnetic Fields. *Journal of Applied Physics*, **61**, 1079-1084. https://doi.org/10.1063/1.338202

[7] Cornils, M. and Paul, O. (2008) Reverse-Magnetic-Field Reciprocity in Conductive Samples with Extended Contacts. *Journal of Applied Physics*, **104**, Article ID: 024505. https://doi.org/10.1063/1.2951895

[8] Carlin, H.J. and Giordano, A.B. (1964) Network Theory: An Introduction to Reciprocal and Nonreciprocal Circuits. Chapter 5, Prentice-Hall, Upper Saddle River, NJ.

[9] Garg, J.M. and Carlin, H.J. (1965) Network Theory of Semiconductor Hall-Plate Circuits. *IEEE Transactions on Circuit Theory*, **12**, 59-73. https://doi.org/10.1109/TCT.1965.1082370

[10] Hofmann, H. (1986) Das elektromagnetische Feld. Springer Verlag Wien, New York. (In German) https://doi.org/10.1007/978-3-7091-4005-5

[11] Kleinman, D.A. and Schawlow, A.L. (1960) Corbino Disk. *Journal of Applied Physics*, **31**, 2176-2187. https://doi.org/10.1063/1.1735520

[12] Vanhamäki, H., Viljanen, A. and Amm, O. (2005) Induction Effects on Ionospheric Electric and Magnetic Fields. *Annales Geophysicae*, **23**, 1735-1746. https://doi.org/10.5194/angeo-23-1735-2005

[13] Buehler, M.G. and Pearson, G.L. (1966) Magnetoconductive Correction Factors for an Isotropic Hall Plate with Point Sources. *Solid-State Electronics*, **9**, 395-407. https://doi.org/10.1016/0038-1101(66)90154-7

[14] Smythe, W.R. (1989) Static and Dynamic Electricity. 3rd Edition, Taylor and Francis, Bristol, PA.

[15] Furlani, E.P. (2001) Permanent Magnet and Electromechanical Devices. Academic Press, San Diego, CA.

[16] Ausserlechner, U. (2018) An Analytical Theory of Piezoresistive Effects in Hall Plates with Large Contacts. *Advances in Condensed Matter Physics*, **2018**, Article ID: 7812743. https://doi.org/10.1155/2018/7812743

[17] Ausserlechner, U. (2017) The Signal-to-Noise Ratio and a Hidden Symmetry of Hall Plates. *Solid-State Electronics*, **135**, 14-23. https://doi.org/10.1016/j.sse.2017.06.007

[18] Midgley, D. (1960) The Possibility of a Self-Sustaining Corbino Disk. *Nature*, **186**, 377. https://doi.org/10.1038/186377a0

[19] Johnson, H.H. and Midgley, D. (1962) The Corbino Disc and Its Self-Magnetic

Field. *Proceedings of the IEE-Part B: Electronic and Communication Engineering*, **109**, 283-286. https://doi.org/10.1049/pi-b-2.1962.0199

[20] Boiko, B.B., Sobol, V.R., Mazurenko, O.N. and Drozd, A.A. (1996) Magnetosensitive Conductivity of Aluminum and the Advantage of Corbino Geometry. In: Summers, L.T., Ed., *Advances in Cryogenic Engineering Materials*, Springer, Boston, MA, 1063-1069. https://doi.org/10.1007/978-1-4757-9059-7_139

[21] Onsager, L. (1931) Reciprocal Relations in Irreversible Processes. II. *Physical Review Journals Archive*, **38**, 2265-2279. https://doi.org/10.1103/PhysRev.38.2265

[22] Miller, D.G. (1960) Thermodynamics of Irreversible Processes: The Experimental Verification of the Onsager Reciprocal Relations. *Chemical Reviews*, **60**, 15-37. https://doi.org/10.1021/cr60203a003

[23] Munter, P.J.A. (1990) A Low-Offset Spinning Current Hall Plate. *Sensors and Actuators A: Physical*, **21**-**23**, 743-746. https://doi.org/10.1016/0924-4247(89)80069-X

[24] Ausserlechner, U. (2004) Limits of Offset Cancellation by the Principle of Spinning Current Hall Probe. *Proceedings of IEEE SENSORS*, Vienna, Austria, 24-27 October 2004, 1117-1120. https://doi.org/10.1109/ICSENS.2004.1426372

[25] Madec, M., Kammerer, J.B., Hébrard, L. and Lallement, C. (2011) Analysis of the Efficiency of Spinning-Current Techniques Thru Compact Modeling. *SENSORS*, 2011 *IEEE*, Limerick, Ireland, 28-31 October 2011, 542-545. https://doi.org/10.1109/ICSENS.2011.6127318

[26] Dowling K.M., Alpert, H.S., Yalamarthy, A.S., Satterthwaite, P.F., Kumar, S., Köck, H., Senesky, D.G., *et al.* (2019) Micro-Tesla Offset in Thermally Stable AlGaN/GaN 2DEG Hall-Effect Plates Using Current Spinning. *IEEE Sensors Letters*, **3**, Article No. 2500904. https://doi.org/10.1109/LSENS.2019.2898157

[27] Van Der Meer, J.C., Riedijk, F.R., van Kampen, E., Makinwa, K.A. and Huijsing, J.H. (2005) A Fully Integrated CMOS Hall Sensor with a 3.65 μT 3 σ Offset for Compass Applications. 2005 *IEEE International Digest of Technical Papers. Solid-State Circuits Conference*, San Francisco, CA, 10-10 February 2005, 246-247.

Appendix A

We compute the potential in a disk-shaped Hall plate with current input at the center point and current exit at the rightmost point (see Figure 3). In this case there exists no stream function but we can still use the ansatz (A1) of part I [1] for the electric potential.

$$\phi = \left(A_0 \ln r + B_0\right)\left(C_0\varphi + 1\right) + \sum_{k=1}^{\infty}\left(A_k r^k + B_k r^{-k}\right)\left(C_k \sin k\varphi + \cos k\varphi\right). \quad \text{(A1)}$$

From periodicity, it follows $C_0 = 0$. With (1) the radial component of the current density becomes:

$$J_r = \boldsymbol{J}\cdot\boldsymbol{n}_r = \frac{-1}{\rho\left(1+\mu_H^2 B_{a,z}^2\right)}\left(\frac{\partial\phi}{\partial r} - \frac{\mu_H B_{a,z}}{r}\frac{\partial\phi}{\partial\varphi}\right) \quad \text{(A2)}$$

with $\boldsymbol{n}_r$ being the unit vector in radial direction. The current flowing out of any circle with $r < 1$ around the current input is given by:

$$t_H \int_{-\pi}^{\pi} J_r r \mathrm{d}\varphi = I_{\text{supply}} \quad \text{(A3)}$$

If we insert (A1) into (A2) into the integrand in (A3) all terms except A_0 vanish and we get:

$$A_0 = -I_{\text{supply}} R_{\text{sheet}}\left(1+\mu_H^2 B_{a,z}^2\right)\Big/(2\pi) \quad \text{(A4)}$$

Next, we evaluate (A2) at the unit circle $r = 1$ and set it equal to the Fourier series of the outflowing current.

$$J_r\left(r=1\right) = \begin{cases} I_{\text{supply}}\big/\left(2\varepsilon t_H\right) & \text{for } -\varepsilon \le \varphi \le \varepsilon \\ 0 & \text{for } \varepsilon \le |\varphi| \end{cases} \quad \text{(A5)}$$

With (A2) and (A1) the radial current density at the unit circle still has odd terms in φ which have to vanish because the current density (A5) has even symmetry. This gives $C_k = -1\big/\left(\mu_H B_{a,z}\right)\ \forall k \ge 1$. For the other coefficients, we get in the limit $\varepsilon \to 0$

$$A_k = I_{\text{supply}} R_{\text{sheet}}\ \mu_H B_{a,z}\big/(k\pi) \quad \forall k \ge 1. \quad \text{(A6)}$$

Grounding the potential at the leftmost point finally gives

$$B_0 = \frac{I_{\text{supply}} R_{\text{sheet}}}{\pi}\sum_{k=1}^{\infty}\frac{(-1)^k}{k} = I_{\text{supply}} R_{\text{sheet}}\frac{-\ln 2}{\pi}. \quad \text{(A7)}$$

With these coefficients, the series in the ansatz can be summed up in closed form and we can express the potential *at applied magnetic field* in terms of elementary functions.

$$\phi = \frac{I_{\text{supply}} R_{\text{sheet}}}{\pi}\left(-\frac{1+\mu_H^2 B_{a,z}^2}{4}\ln\left(x^2+y^2\right) + \frac{1}{2}\ln\left(\frac{(1-x)^2+y^2}{4}\right) + \mu_H B_{a,z}\arctan\frac{y}{1-x}\right) \quad \text{(A8)}$$

The first two terms give ϕ_{even} analogous to (2b), the third term is the Hall potential ϕ_H according to (2c). It agrees perfectly with Figure 3(c). ϕ_{even} contains second order terms in $B_{a,z}$, which is in contrast to (22) of part I. Conversely, ϕ_H is linearly proportional to $B_{a,z}$, which agrees with the Hall potential in part I (see (17a) in part I).

In the above derivation, we differentiated the series expansion of the ansatz term wise to obtain (A6). This was not allowed on the unit circle, because there the series diverges for $\varepsilon \to 0$. The situation improves if we keep ε finite for the boundary conditions and compute $\varepsilon \to 0$ afterwards in the potential ϕ. Alternatively, we can simply check if the result (A8) fulfills Laplace's equation and all boundary conditions, which it does.

The stagnation point of the spiral current streamlines is defined by $\left|\boldsymbol{J}\left(r_S, \varphi_S\right)\right| = 0$. The radial current density vanishes everywhere on the unit circle except at the current contact. The azimuthal current density vanishes also in one point on the unit circle which is defined by:

$$J_\varphi = \boldsymbol{J}\cdot\boldsymbol{n}_\varphi = \frac{-1}{\rho\left(1+\mu_H^2 B_{a,z}^2\right)}\left(\frac{1}{r}\frac{\partial\phi}{\partial\varphi} + \mu_H B_{a,z}\frac{\partial\phi}{\partial r}\right) \to 0 \quad \text{for } r = 1 \tag{A9}$$

Inserting (A8) into (A9) gives:

$$\varphi_S = 2\arctan\left(\frac{1}{\mu_H B_{a,z}}\right) = \operatorname{sgn}\left(\theta_H\right)\pi - 2\theta_H \tag{A10}$$

In Figures 3(a)-(e) it appears that with increasing Hall angle the current streamlines encircle the input current contact more often. However, this is only a deception caused by the finite mesh of the numerical simulation as the following arguments show. The outmost current streamline flows on the unit circle during its last loop (this is the red streamline in Figure 7). If we follow it backwards from the current sink towards the input contact, it will cross the negative x-axis several times: at $x_0 = -1, x_1 = -1+\Delta_1, x_2 = -1+\Delta_1+\Delta_2, \cdots$. If we in-

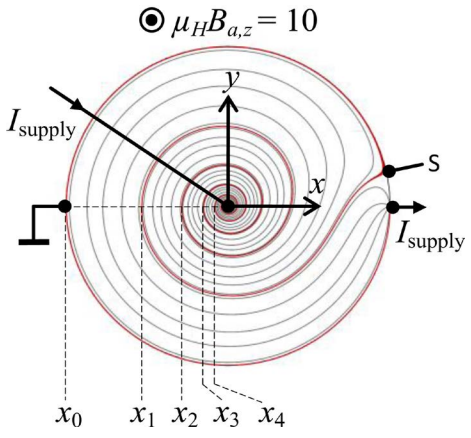

Figure 7. A simply-connected circular Hall disk from Figure 3(b) with point supply contact in its center. Several current streamlines are shown in grey color. The outmost current streamline is shown in red: it flows from the stagnation point S in CCW direction along the perimeter to the current output contact.

tegrate the current density between two neighboring crossings it must give the entire supply current. We define the spacing Δ_n between n-th and $(n+1)$-th crossing by

$$t_H \int_{x=x_n}^{x_n+\Delta_n} J_y(x, y=0)\,\mathrm{d}x = -I_{\text{supply}} \tag{A11}$$

with $x_{n+1} = x_n + \Delta_n$ and $x_1 = -1$. With $t_H J_y(x, y=0) = I_{\text{supply}} \mu_H B_{a,z} / (2\pi x)$ we get after some manipulation

$$\Delta_n = \left(1 - \exp\left(\frac{-2\pi}{\mu_H B_{a,z}}\right)\right) \exp\left(\frac{-2\pi(n-1)}{\mu_H B_{a,z}}\right) \tag{A12a}$$

$$x_N = -1 + \sum_{n=1}^{N} \Delta_n = -\exp\left(\frac{-2\pi N}{\mu_H B_{a,z}}\right) \tag{A12b}$$

This means that the spacing between consecutive loops of the current streamlines gets smaller and smaller the more they approach the current input contact while the current density goes to infinity. In other words, every current streamline encircles the origin infinitely often, regardless if the magnetic field is weak or strong. The only difference is that at weak magnetic field the loops are much closer to the origin than at strong magnetic field. For a weak magnetic field with $\mu_H B_{a,z} = 0.1$ one gets

$$x_0 = -1, x_1 \cong -5.2\times10^{-28}, x_2 \cong -2.7\times10^{-55},$$
$$x_3 \cong -1.4\times10^{-82}, x_4 \cong -7.1\times10^{-110}, \cdots.$$

whereas for a strong magnetic field with $\mu_H B_{a,z} = 10$ one gets

$$x_0 = -1, x_1 \cong -0.53349, x_2 \cong -0.28461, x_3 \cong -0.15184, x_4 \cong -0.08100, \cdots$$

It also means that the current flowing across the line segment defined by the points $(x, y) = (-1, 0)$ and $(x, y) = (0, 0)$ is infinite even at arbitrarily weak non-vanishing magnetic field. *A passive device, which is supplied by finite current, develops infinite circulating current*. The power dissipation is already infinite at zero applied magnetic field due to the point-sized supply contacts, yet it has one additional infinite term proportional to the square of $B_{a,z}$.

There is a remarkable difference between zero and non-zero $B_{a,z}$. At zero applied magnetic field the current streamlines do not encircle the origin. However, only a minute $B_{a,z}$ already changes the pattern of streamlines drastically by creating infinitely many spiral turns around the origin. Of course, here we face a gap between our simple theory and physical experience, because point-sized contacts are only hypothetical and in case of such huge current densities one would have to account for new interactions such as the magnetic field of current streamlines on their neighbors.

This self-field phenomenon was studied in Corbino disks in [11] [18] [19]. There it was explained that the self-field adds *constructively* to the applied magnetic field if the charge carriers flow inward, and *destructively* if they flow outward. This holds for both polarities of charge carriers, current, and applied

magnetic field. If the inner contact of such a corbinotron shrinks to zero the total magnetic field and current near its center are identical to our Figure 7. An approximate solution is given in [11].

$$B_{sf,z} \cong B_{a,z}\left(\left(\frac{r_2}{r}\right)^{\mu_0\mu_H I_{\text{supply}}/(4\pi r_2)} - 1\right) \quad \text{for} \quad r \ll r_2 \tag{A13}$$

where $B_{sf,z}$ is the flux density generated by the current through the disk ("self field"), $B_{a,z}$ is the applied magnetic flux density, μ_0 is the permeability of free space, and r_2 is the outer radius of the disk. In the destructive case, $\mu_H I_{\text{supply}} < 0$ the total magnetic field vanishes in the center $B_{sf,z} + B_{a,z} \to 0$. According to Section 2 μ_H becomes negative for positive charge carriers. In the constructive case $\mu_H I_{\text{supply}} > 0$ the total magnetic field in the center goes to infinity $B_{sf,z} + B_{a,z} \to \text{sgn}\left(B_{a,z}\right) \times \infty$ even if the applied magnetic field is very weak and the Hall mobility and supply current are very small. In other words, the self-field increases the vorticity around the center contact for the constructive case, while it reduces it for the destructive case. In [11] [18] [19] [20], the authors discuss if this mechanism can be used in diodes, inductors, and energy storages.

If the point of the current input contact is not in the origin but somewhere else inside the unit disk, we can use a Möbius (bilinear) transformation to conformally map the unit disk on itself and the input contact onto the origin. If the Hall plate has some other simply-connected shape than a disk, there is always some conformal mapping onto the unit disk. If the current output is not on the outer perimeter, but also inside the unit disk, we can replace the problem by a superposition of two disks, where one disk has a current input contact on the unit circle and the other disk has a current output contact at the same location. A general formula for all these cases can be found in [13].

Appendix B

If we cut out a circular hole around the origin and inject the current in any point on this insulating hole boundary, the current streamlines will not encircle the origin infinitely many times any more. The ring-shaped conductive region in Figure 8 has an inner radius r_1 and an outer radius 1. Current is injected in point $(x,y) = (r_1, 0)$ and extracted at $(x,y) = (1,0)$. Point $(x,y) = (-1,0)$ is grounded. With the ansatz (A1) we get $C_0 = 0$ and A_0 is given by (A4). The radial current density has to be an odd function in φ on $r = r_1$ and $r = 1$. This gives two equations for the unknowns A_k, B_k, C_k. If we develop the current density on $r = 1$ into a Fourier series like in (A5), we get the third equation. We do not compute the limit $\varepsilon \to 0$ here, because finite ε improves the convergence of the series for $J_r(r = 1, \varphi)$. Solution of this set of three equations gives two sets of solutions:

The first solution is $A_k = -I_{\text{supply}} R_{\text{sheet}} \sin(\varepsilon k)/(\pi\varepsilon k^2), B_k = 0, C_k = -\mu_H B_{a,z}$.

The second solution is $A_k = 0, B_k = I_{\text{supply}} R_{\text{sheet}} \sin(\varepsilon k)/(\pi\varepsilon k^2), C_k = \mu_H B_{a,z}$.

Both solutions do not give the correct radial current density on the inner circle

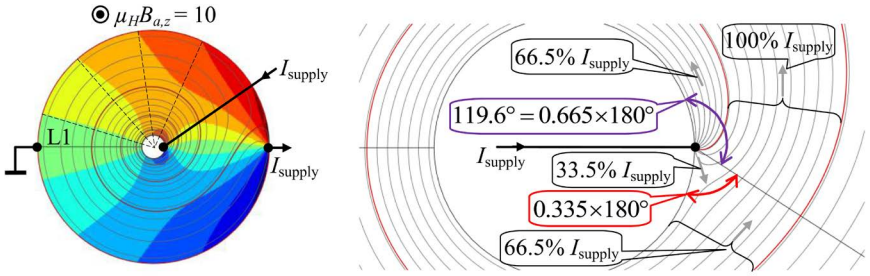

(a) (b)

Figure 8. A circular Hall disk with a central circular hole. The hole is ten times smaller than the disk. (a) The color mapping shows the Hall geometry factor $G_H(r,\varphi) = \phi_H(r,\varphi) \big/ \left(I_{\text{supply}} R_{sheet} \tan\theta_H\right)$ (red is +1, blue is −1). Several current streamlines are shown in grey color. The outmost current streamline is shown in red. For $\mu_H B_{a,z} = 10$ it encircles the hole $N_{turns} = 3.665$ times. The dashed lines in radial directions show that the Hall potential at the unit circle is identical to the Hall potential at the hole boundary at fixed azimuthal angle. (b) Close-up of the current streamlines at the input contact. The outmust current streamline in red exits the current contact at an angle of $180^\circ \times \left(N_{turns} - \lfloor N_{turns} \rfloor\right) = 119.6^\circ$ to the hole boundary. The figure shows the balance of currents (Kirchhoff's nodal rule) near the input contact.

$r = r_1$. However, a linear combination of both solutions gives the correct radial current density. Thereby the first solution is multiplied by $\left(1 + r_1^k\right)^{-1}$ and the second solution is multiplied by $r_1^k \left(1 + r_1^k\right)^{-1}$. The last unknown B_0 is obtained by grounding the potential. Finally, we can perform the limit $\varepsilon \to 0$ for the potential. This gives

$$\phi = \frac{I_{\text{supply}} R_{\text{sheet}}}{\pi} \left\{ -\frac{1+\mu_H^2 B_{a,z}^2}{2} \ln r + \sum_{k=1}^{\infty} \frac{(-1)^k - (-r_1)^k + \left(-r^k + (r_1/r)^k\right)\cos k\varphi}{k\left(1+r_1^k\right)} \right.$$
$$\left. + \mu_H B_{a,z} \sum_{k=1}^{\infty} \frac{r^k + (r_1/r)^k}{k\left(1+r_1^k\right)} \sin k\varphi \right\} \tag{B1}$$

The last term in (B1) is the Hall potential, which is again linear in applied magnetic field. The square law dependence of ϕ_{even} on the applied magnetic field is identical to **Appendix A**. On the hole boundary and on the outer perimeter it holds

$$\phi_H(r = r_1) = \phi_H(r = 1) = \frac{I_{\text{supply}} R_{\text{sheet}}}{2} \mu_H B_{a,z} \left(\text{sgn}(\varphi) - \frac{\varphi}{\pi}\right) \tag{B2}$$

Obviously, it is not constant versus φ on the boundaries. In $r = 1$ the Hall potentials of **Figure 7** and **Figure 8** are identical – the hole does not change them. Moreover, the Hall voltage between a point on the outer perimeter and a point on the hole boundary vanishes, if both points are at the same azimuthal angle. With (B1) and (1) we get the odd current density, which flows in concentric circles around the hole.

$$\frac{\boldsymbol{J}(B_{a,z}) - \boldsymbol{J}(-B_{a,z})}{2} = \boldsymbol{J}_{\text{odd}} = \frac{I_{\text{supply}}}{t_H} \frac{\mu_H B_{a,z}}{2\pi r} \boldsymbol{n}_\varphi \tag{B3a}$$

Both curl and divergence of the odd current density vanish in $0<r\le 1$: $\nabla\cdot\boldsymbol{J}_{\text{odd}}=0$, $\nabla\times\boldsymbol{J}_{\text{odd}}=\boldsymbol{0}$. Yet, the circulation around the point of current input does not vanish:

$$\Gamma=\oint\boldsymbol{J}_{\text{odd}}\cdot\mathrm{d}\boldsymbol{s}=\int_{\varphi=-\pi}^{\pi}\boldsymbol{n}_{\varphi}\cdot\boldsymbol{J}_{\text{odd}}(r,\varphi)r\mathrm{d}\varphi=\frac{I_{\text{supply}}}{t_H}\mu_H B_{a,z} \tag{B3b}$$

Equation (B3b) is in accordance with (17a). In this example, Stokes integral theorem does not apply $\oint\boldsymbol{J}_{\text{odd}}\cdot\mathrm{d}\boldsymbol{s}\neq\int\nabla\times\boldsymbol{J}_{\text{odd}}\cdot\mathrm{d}\boldsymbol{A}$, because $\boldsymbol{J}_{odd}$ is not continuous at $r=0$ (its y-component jumps from negative infinite to positive infinite along the x-axis through the origin). Note that this singular point is outside the conductive region but still inside the closed curve. With (14a, b) the loop stream function is

$$\psi_{\text{loop}}=I_{\text{supply}}R_{\text{sheet}}\mu_H B_{a,z}\frac{\ln r}{2\pi} \tag{B4}$$

It is constant on the hole boundary and it vanishes on the outer perimeter (= the unit circle). It does not depend on the size of the hole. Therefore (B4) also applies to the Hall plates of Figure 3 and Figure 7 which have no hole.

Comparing (B1) with (B4) asserts (19). From (B1) we get

$$\boldsymbol{J}_0=\frac{I_{\text{supply}}}{2\pi r t_H}\left((1+2\Sigma_C)\boldsymbol{n}_r-2\Sigma_S\boldsymbol{n}_{\varphi}\right) \tag{B5a}$$

with the abbreviations

$$\Sigma_C=\sum_{k=1}^{\infty}\frac{r^k+(r_1/r)^k}{1+r_1^k}\cos k\varphi\quad\text{and}\quad\Sigma_S=\sum_{k=1}^{\infty}\frac{r^k-(r_1/r)^k}{1+r_1^k}\sin k\varphi\,. \tag{B5b}$$

If all boundaries are electrodes the device is a Corbino disk with current density at zero applied magnet field

$$\tilde{\boldsymbol{J}}_0=\frac{I_{\text{supply}}}{2\pi r t_H}\boldsymbol{n}_r \tag{B5d}$$

From (B1) we get

$$\nabla\phi_H=\frac{I_{\text{supply}}}{\pi r t_H}\rho\mu_H B_{a,z}\left(\Sigma_S\boldsymbol{n}_r+\Sigma_C\boldsymbol{n}_{\varphi}\right) \tag{B5e}$$

Finally, with (B5a-e) we see that the gradient of the Hall potential is orthogonal to the streamlines of $\boldsymbol{J}_0-\tilde{\boldsymbol{J}}_0$,

$$\left(\boldsymbol{J}_0-\tilde{\boldsymbol{J}}_0\right)\cdot\nabla\phi_H=\left(\frac{I_{\text{supply}}}{\pi r t_H}\right)^2\rho\mu_H B_{a,z}\left(\Sigma_C\boldsymbol{n}_r-\Sigma_S\boldsymbol{n}_{\varphi}\right)\cdot\left(\Sigma_S\boldsymbol{n}_r+\Sigma_C\boldsymbol{n}_{\varphi}\right)=0 \tag{B5f}$$

and therefore the Hall potential is constant along the streamlines of $\boldsymbol{J}_0-\tilde{\boldsymbol{J}}_0$.

With (16) we can compute the total circulating current, if point 2 is at the current input and point 1 is at the perimeter. It is equal to $-\psi_{\text{loop}}(r=r_1)/R_{\text{sheet}}\propto|\ln r_1|$. Therefore the circulating current is finite for $r_1>0$ and it is infinite if the size of this hole goes to zero (however, this divergence is only logarithmically and therefore weak). Then the loop stream function has an isolated singularity at the

central point current contact. We define the number of CCW loops N_{loops} of the streamlines around the hole by

$$I_{\text{loop},12} = \frac{\psi_{\text{loop},1} - \psi_{\text{loop},2}}{R_{\text{sheet}}} = -t_H \int_{x=-1}^{-r_1} J_y\left(y=0\right)\mathrm{d}x = N_{\text{loops}} I_{\text{supply}} \tag{B6a}$$

whereby point 2 is the positive supply contact at $(r,\varphi)=(r_1,0)$ and point 1 is the negative one at $(r,\varphi)=(1,0)$. This gives

$$N_{\text{loops}} = \mu_H B_{a,z}\left(-\ln r_1\right)/(2\pi) \tag{B6b}$$

In Figure 8(a) the current through the black line L1 left of the hole is $3.664679\times I_{\text{supply}}$ for $\mu_H B_{a,z}=10$ and this means that the streamlines encircle the hole 3.665 times. The non-integer value comes from the outmost streamline (in red color), which flows along the perimeter between the outer stagnation point and the current output contact. At the current input contact there is an angle of $180^\circ\times\left(N_{\text{turns}}-\lfloor N_{\text{turns}}\rfloor\right)$ between this red streamline and the hole boundary, and therefore a current equal to $I_{\text{supply}}\times\left(N_{\text{turns}}-\lfloor N_{\text{turns}}\rfloor\right)$ flows in the innermost turn of the spiral around the hole (see Figure 8(b)). $\lfloor N_{\text{turns}}\rfloor$ denotes the truncated value of N_{turns}. If we start at zero applied magnetic field, the tangent on the red streamline in the input contact has positive infinite slope. With rising $B_{a,z}$ the slope decreases to negative infinite slope. At $\mu_H B_{a,z}=-2\pi/\ln r_1$ its slope jumps to positive infinite again and the game repeats until the magnetic field has doubled. Hence, the slope of the tangent jumps at integer multiples of $B_{a,z}=-2\pi/(\mu_H \ln r_1)$ and with every jump the spiral grows by one additional turn and the outer stagnation point moves CW from 180˚ towards 0˚ with decreasing speed (see also Figure 9).

The spiral current pattern in Figure 9 has two stagnation points, one on the outer perimeter and one on the inner hole boundary. Since $\boldsymbol{J}=\boldsymbol{0}$ in the

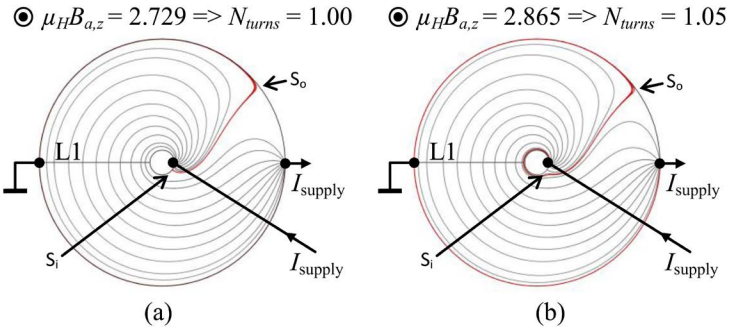

Figure 9. The circular Hall disk with a central circular hole from Figure 8. In (a) the applied magnetic field has exactly such a value that the outmost current streamline (in red color) has negative infinite slope at the current input contact. The red streamline flows from the input contact CW along the hole boundary to the inner stagnation point S_i, where it leaves the hole boundary, crosses the annular region until it reaches the outer boundary in the outer stagnation point S_o. Then it flows along the outer boundary CCW towards the current sink. In (b) the magnetic field is increased by 5% so that the slope of the tangent snaps back to a large positive value and the red streamline encircles the hole CCW one time until it meets the inner stagnation point S_i from where its journey is identical to (a). Several other streamlines are shown in grey color.

stagnation points, also $\boldsymbol{E}$ vanishes there and ϕ has a saddle point. With $\partial\phi/\partial\varphi = 0$ and the symmetry of (B1) it follows that the stagnation point on the inner boundary occurs at $\varphi = -\varphi_S$ if the stagnation point on the outer boundary is at $\varphi = \varphi_S$.

With (B6b) we can estimate how small the hole must be that the streamlines encircle it at least once: for a magnetic field with $\mu_H B_{a,z} = 0.1$ (5.7° Hall angle; this is a flux density of roughly 0.9 T in low n-doped silicon) the hole must have a radius r_1 smaller than 5.2×10^{-28}. It means that for a Hall plate as large as the universe the hole must be smaller than 6 cm. If this Hall plate had no hole the current spiral around its center point contact would have infinitely many turns within a circle with 6 cm diameter but only a single turn outside on its way to the end of the universe. If the applied magnetic field is only 100 times larger we need a disk of only 11.3 cm diameter with a 6 cm hole to observe one turn of the current streamlines. Hence, the effect is extremely sensitive to the strength of the applied magnetic field.

Appendix C

The principle of reverse magnetic field reciprocity (RMFR) from [5] [6] [7] is a very powerful tool, which we used several times. But we have to take care if it is valid in two-dimensional (2D) multiply-connected regions, because in [6] [7] the authors used $\nabla\cdot\boldsymbol{J} = 0$ to prove it for 3D regions, however, in 2D regions with internal current sources we have $\nabla\cdot\boldsymbol{J} \neq 0$ (see (13)). The two reciprocal operating conditions are sketched in **Figure 10** with positive applied magnetic field $B_{a,z} > 0$ in **(a)** and negative one $B_{a,z} < 0$ in **(b)**. Thereby contact 4 is an internal current source in **(b)**. Following [6] we write

$$\int_V \nabla\cdot\left(\phi^a\boldsymbol{J}^b - \phi^b\boldsymbol{J}^a\right)\mathrm{d}V = \int_V \left(\boldsymbol{J}^a\cdot\boldsymbol{E}^b - \boldsymbol{J}^b\cdot\boldsymbol{E}^a\right) + \phi^a\nabla\cdot\boldsymbol{J}^b - \phi^b\nabla\cdot\boldsymbol{J}^a\mathrm{d}V \quad \text{(C1)}$$

The superscripts a, b denote quantities which occur in **Figure 10(a)** & **Figure 10(b)**. With (1) it follows $\boldsymbol{J}^b\cdot\boldsymbol{E}^a = \boldsymbol{J}^a\cdot\boldsymbol{E}^b$ if we use $\boldsymbol{B}_a^a = -\boldsymbol{B}_a^b$. This is a consequence of the odd symmetry of the resistivity tensor in (1) of part I, which was proven under general thermodynamic assumptions in [21] after a long lasting

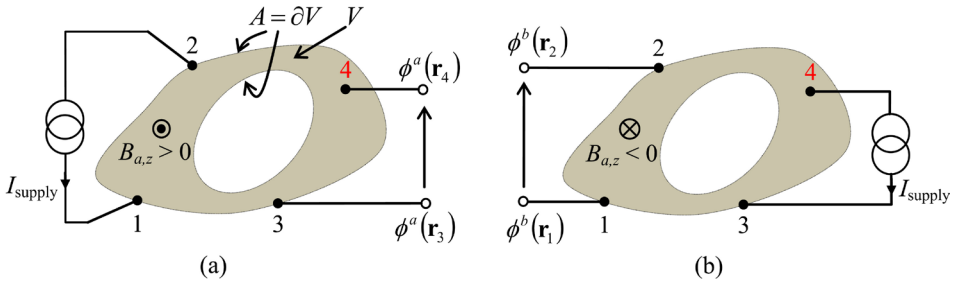

Figure 10. Reverse magnetic field reciprocity principle (RMFR) for a doubly connected plane Hall plate with the interior contact 4. In (a) the applied magnetic field is positive. In (b) it is negative. In (a) and (b) inputs and outputs are swapped. The output voltage is identical for constant supply current, if the perpendicular applied magnetic field changes its sign: $\phi^a(\boldsymbol{r}_3) - \phi^a(\boldsymbol{r}_4) = \phi^b(\boldsymbol{r}_1) - \phi^b(\boldsymbol{r}_2)$.

dispute in the early 20th century [22]. We set $\nabla\cdot\boldsymbol{J}^a=-I_{\text{supply}}\delta(\boldsymbol{r}-\boldsymbol{r}_2)+I_{\text{supply}}\delta(\boldsymbol{r}-\boldsymbol{r}_1)$ and $\nabla\cdot\boldsymbol{J}^b=-I_{\text{supply}}\delta(\boldsymbol{r}-\boldsymbol{r}_4)+I_{\text{supply}}\delta(\boldsymbol{r}-\boldsymbol{r}_3)$. Then (C1) equates to $-I_{\text{supply}}\phi^a(\boldsymbol{r}_4)$. Contacts 1, 2, 3 do not contribute to the volume integral, because they are not *inside* the volume but only on its boundary. If $\phi^a\boldsymbol{J}^b-\phi^b\boldsymbol{J}^a$ is continuously differentiable in a neighborhood of the conductive region we can apply Gauss' integral theorem to the LHS of (C1). This gives

$$\oint_{A=\partial V}\left(\phi^a\boldsymbol{J}^b-\phi^b\boldsymbol{J}^a\right)\cdot\mathrm{d}\boldsymbol{A}=-I_{\text{supply}}\phi^a(\boldsymbol{r}_3)-\left[I_{\text{supply}}\phi^b(\boldsymbol{r}_2)-I_{\text{supply}}\phi^b(\boldsymbol{r}_1)\right] \quad \text{(C2)}$$

whereby contact 4 is not on the closed boundary. Comparison of (C1) and (C2) gives the RMFR principle: $\phi^a(\boldsymbol{r}_3)-\phi^a(\boldsymbol{r}_4)=\phi^b(\boldsymbol{r}_1)-\phi^b(\boldsymbol{r}_2)$.

If contact 4 is not inside the conductive region but on a hole boundary we have the same divergence of $\boldsymbol{J}^b$ as above. Now contacts 3 *and* 4 are on boundaries and so the divergence of $\boldsymbol{J}^b$ does not contribute to the volume integral, however, both contacts contribute to the surface integral. This gives again $\phi^a(\boldsymbol{r}_3)-\phi^a(\boldsymbol{r}_4)=\phi^b(\boldsymbol{r}_1)-\phi^b(\boldsymbol{r}_2)$. Thus, if we assign contact 4 to the hole boundary its contribution shows up in the surface integral (C2), and if we assign it to the interior of the conductive region it contributes to the volume integral (C1), but in both cases, we get the same result. Therefore in [5] the author assigned all current sources and sinks to the interior. Currents through boundaries were replaced by interior point contacts which are infinitely close to the boundary.

To sum up, *the RMFR principle also holds for multiply-connected plane* 2*D regions*.

In a spinning current Hall scheme a Hall plate is operated in a first operating phase according to **Figure 10(a)** and in a second operating phase according to **Figure 10(b)**, however, both times the *same* magnetic field is applied. The output voltages of both phases are sampled and *subtracted* [23] [24] [25]. The result is twice the Hall voltage V_H while any offset voltage V_{even} is removed. In practice this procedure has an outstanding efficiency: it reduces residual zero point errors of Hall plates by nearly three orders in magnitude [26] [27]. That is why it is used pervasively in contemporary smart Hall sensors for automotive and industrial applications, exceeding 100 million parts per year.